

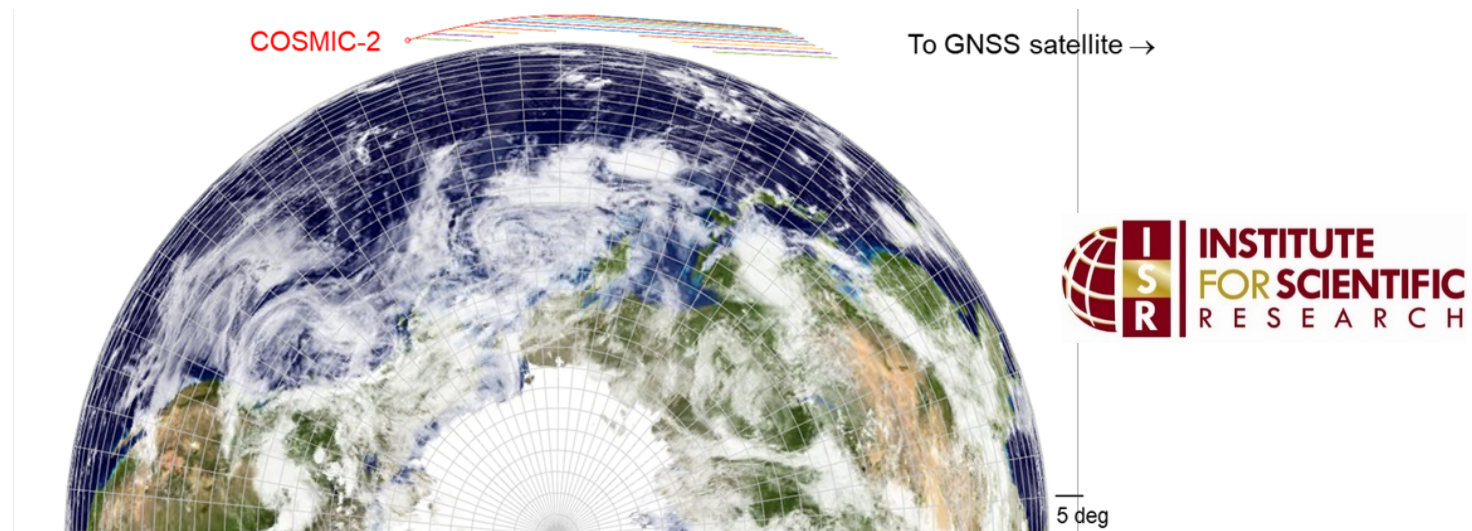
Real-Time Monitoring of Ionospheric Irregularities using Radio Occultation Data

Charles S Carrano¹, Keith M Groves¹, Charles L Rino¹, William J McNeil¹,
Ronald G Caton² and Paul R Straus³

(1) Boston College, Institute for Scientific Research, Chestnut Hill, MA

(2) Air Force Research Lab, Space Sensors Directorate, Kirtland AFB, NM

(3) Aerospace Corp, Los Angeles, CA



African Capacity Building Workshop on Space Weather Effects on GNSS
ICTP, Trieste, 3-14 October 2022



- Radio occultations (RO) are widely used for remote sensing tropospheric parameters and to provide ionospheric electron density profiles for terrestrial and space weather forecasts.
- Radio occultations have also been used to investigate the **morphology of ionospheric irregularities** that cause radio wave scintillation.
- Space based monitoring of ionospheric irregularities is advantageous because it can be performed **continuously and globally**, including over ocean regions not easily monitored with ground based instruments.
- The COSMIC-2 satellites (6 in low inclination orbit) have the **TGRS sensor** for this purpose, which measures high-rate amplitude and phase fluctuations of the GPS and GLONASS L1 and L2 signals.

- Unlike RO retrievals of slant TEC which are dominated by the contribution from close to the tangent point (TP), scintillation can be generated by irregularities located **anywhere along the propagation path**.
- The propagation path of an occultation through the ionosphere can be **very** long (thousands of km). Quantitative use of data requires **geolocation**: determination of the location & spatial extent of the irregularities from the scintillations they produce.
- Under the COSMIC-2 Cal/Val program, we developed the **TGRS Geolocation Product** to geolocate irregularities that produce scintillation of GPS and GLONASS signals. A **Bubble Map Product** depicts bubble boundaries and a **Limb to Disk Product** estimates scintillation strength along vertical propagation paths.

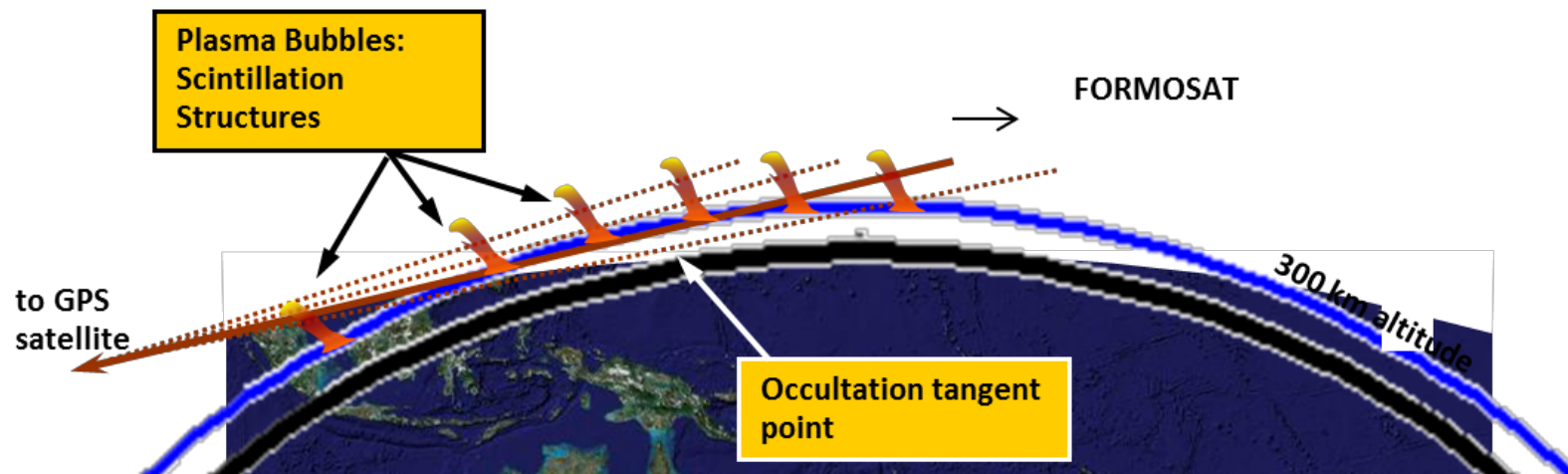
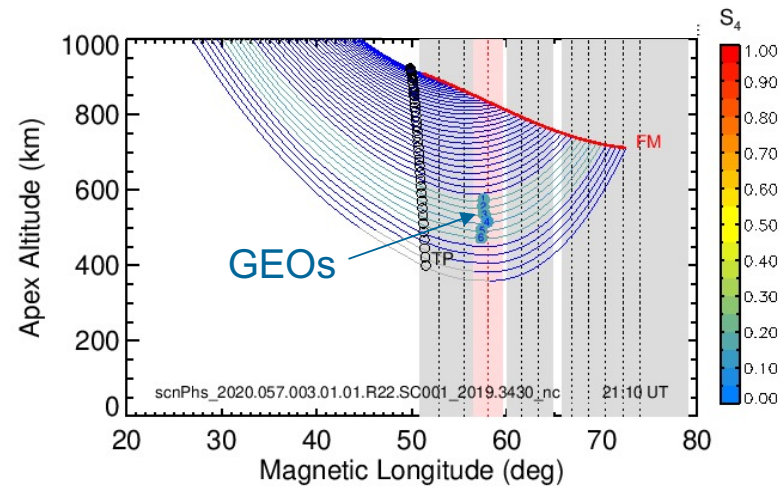
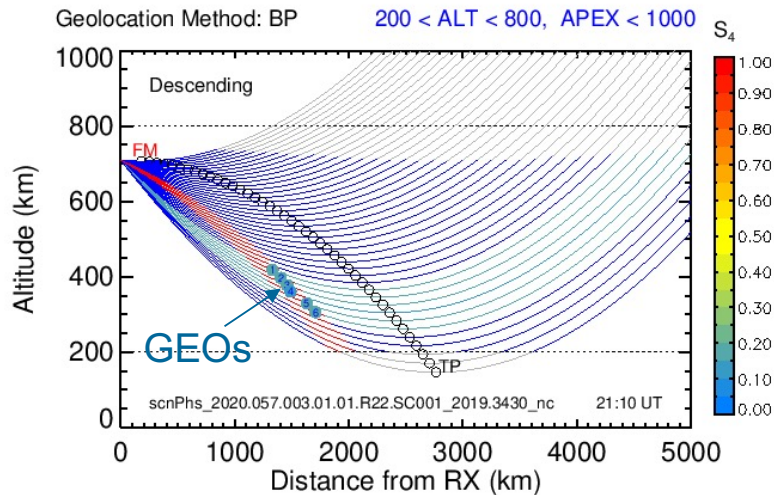
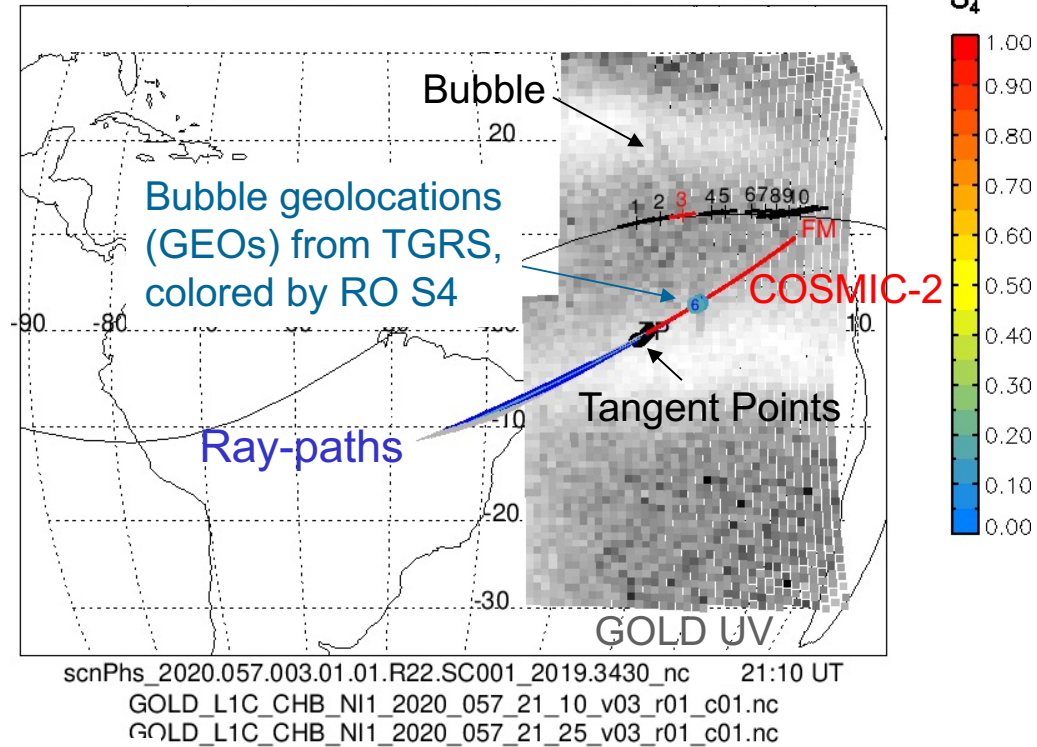
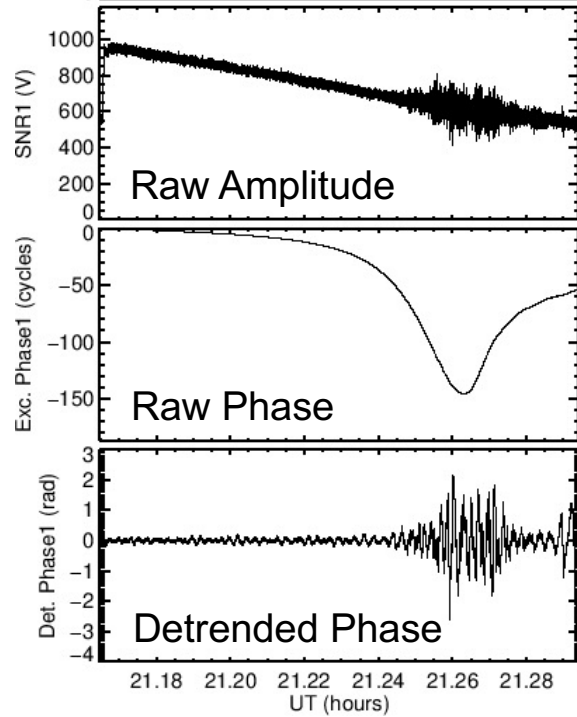


Figure Credit: Ron Caton (AFRL)

Drawn to scale

Bubble Geolocation with COSMIC-2



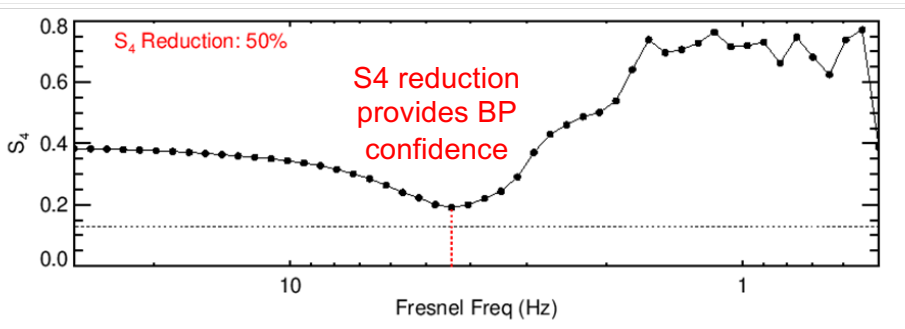
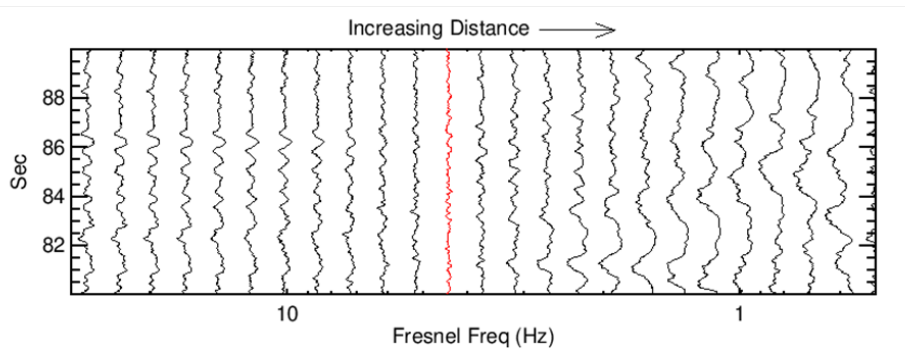
Bubble Geolocation via Back-Propagation



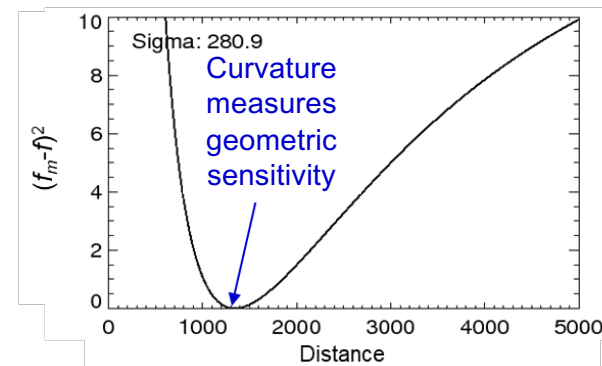
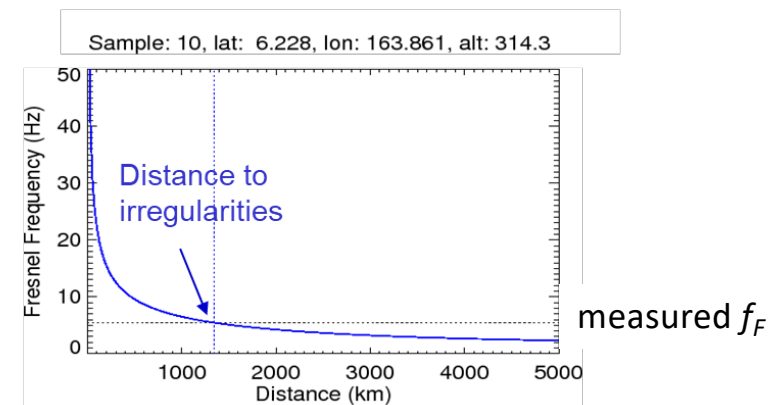
We geolocate the irregularities via back-propagation in the **time domain**, with Fresnel frequency as the independent variable to be measured. We use the Rino scintillation model (1979), generalized to the RO geometry, to relate Fresnel frequency to Fresnel scale, and then to distance along the ray-path to the irregularity region.

$$U_s(t) = F^{-1} \left\{ \exp \left[-\frac{1}{2} i (2\pi f / f_F)^2 \right] F [U_{RX}(t)](f) \right\}$$

1. Back-propagate complex signal in 10-sec segments to measure Fresnel frequency of the scattering.

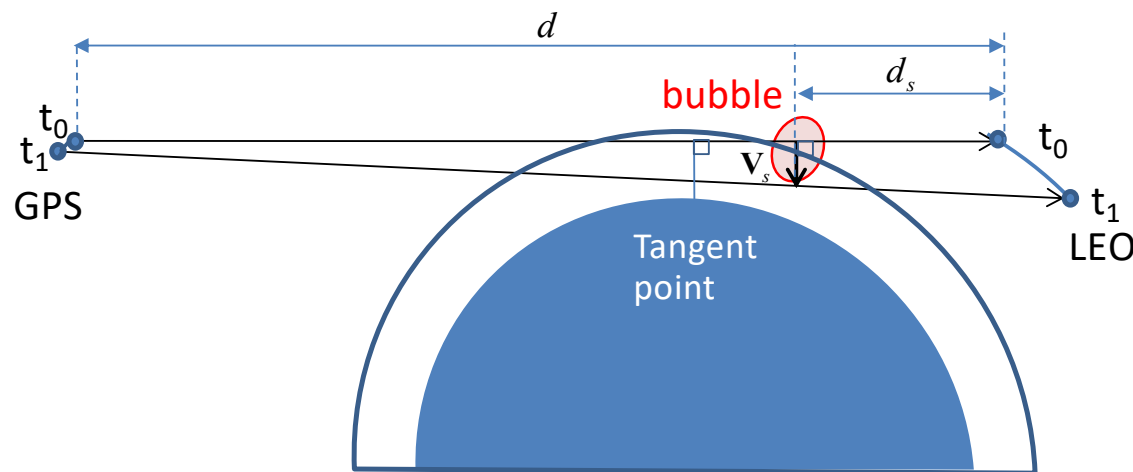


2. Geometric model provides Fresnel frequency vs distance. Intersection with measurement gives distance to irregularities.



- Scan velocity is proportional to distance (d_s) from the irregularities causing the scintillation

$$\mathbf{V}_s(d_s) = \mathbf{V}^{\text{LEO}} + (d_s/d) [\mathbf{V}^{\text{GPS}} - \mathbf{V}^{\text{LEO}}]$$



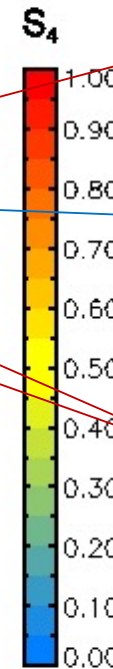
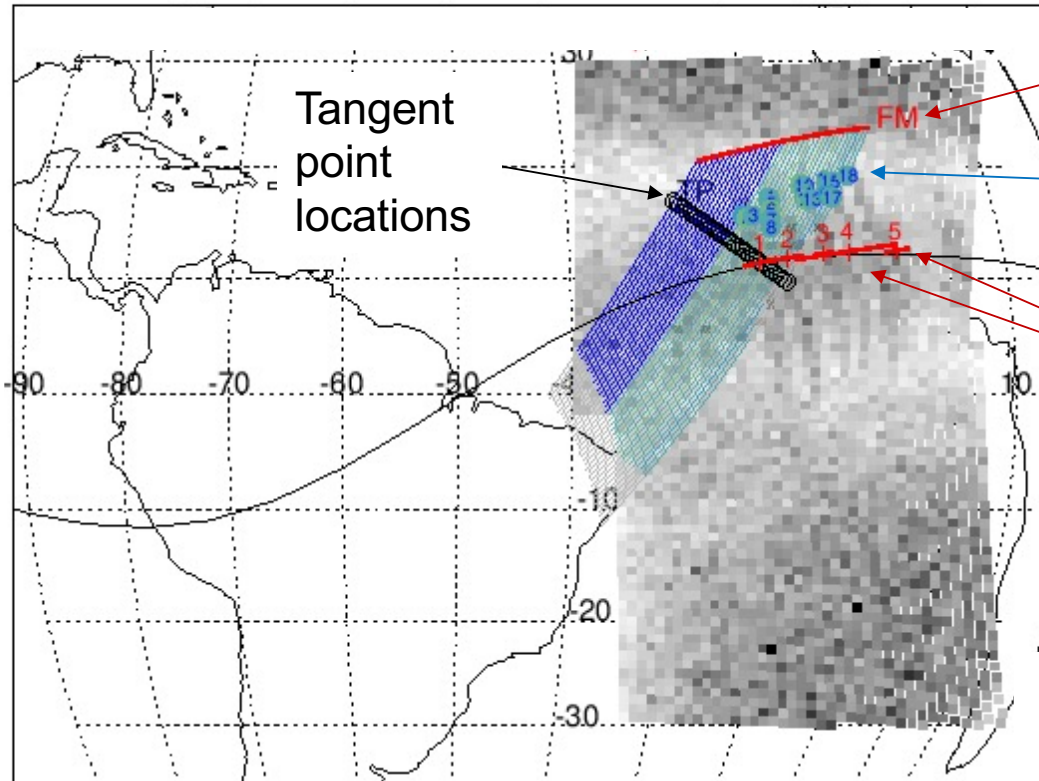
- For anisotropic field-aligned irregularities we must use an effective scan velocity, V_{eff}

• Effective scan velocity: $V_{\text{eff}}(d_s) = \left[\frac{CV_{sx}^2 - BV_{sx}V_{sy} + AV_{sy}^2}{AC - B^2/4} \right]^{1/2}$ V_{sx}, V_{sy} are components of V_s in plane \perp to ray-path

• Fresnel frequency: $f_F(d_s) = V_{\text{eff}} / \rho_F(d_s)$

• Fresnel scale: $\rho_F = \sqrt{\frac{d_R}{k}}, \quad d_R = \frac{(d - d_s)d_s}{d}$

Once $f_F(d_s)$ has been measured, this purely geometric model can be inverted to find d_s



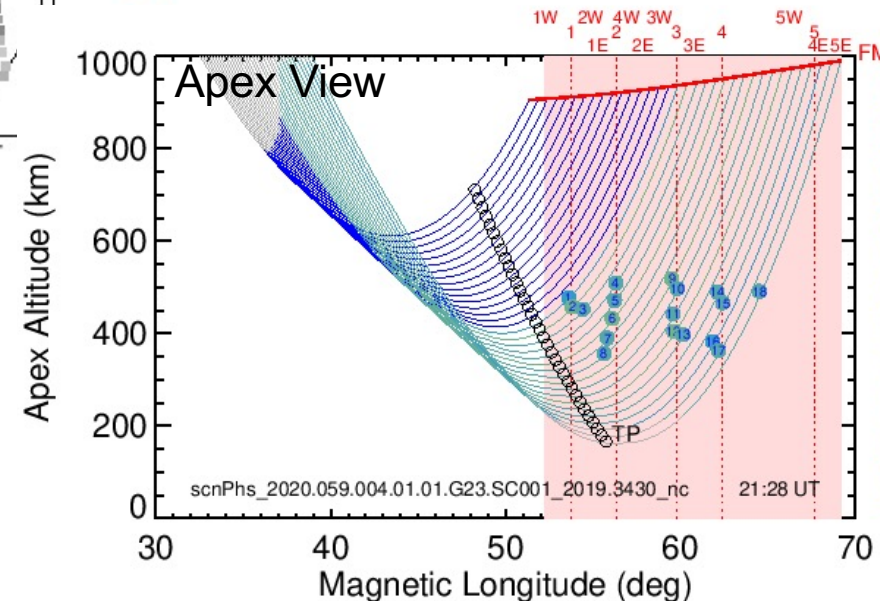
COSMIC-2 orbit

Bubble geolocations (GEOs) from TGRS, colored by RO S_4

Bubbles identified in GOLD UV image

scnPhs_2020.059.004.01.01.G23.SC001_2019.3430_nc 21:28 UT
 GOLD_L1C_CHB_NI1_2020_059_21_40_v03_r01_c01.nc
 GOLD_L1C_CHB_NI1_2020_059_21_25_v03_r01_c01.nc

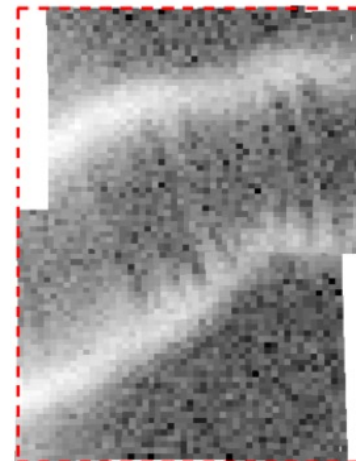
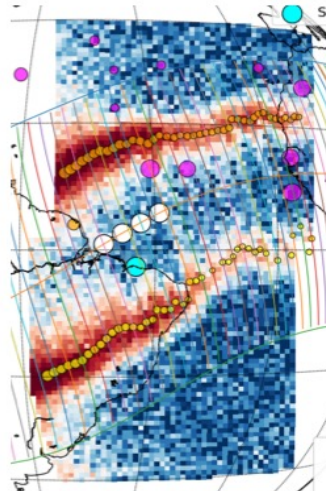
- A single occultation can produce **many GEOs**.
- TGRS does not detect *all* bubbles, however, only those intersected by the RO ray-paths at F-region altitudes, and those for which RO S_4 triggers download of high-rate data.



- GOLD is a NASA-sponsored scanning far ultraviolet (FUV) instrument hosted on a geosynchronous communications satellite in the S. America/Atlantic sector
- On the nightside, GOLD provides images of the O+ 135.6 nm recombination emission (proportional to the square of electron density) at a 15-minute cadence
- Depletions (dark regions) in the 135.6 nm images indicate the presence of equatorial plasma bubbles (EPBs) that often contain irregularities that produce scintillation
- The Cal/Val team employs a 2-step process to obtain EPB information from GOLD
 - UCAR developed an automated algorithm to extract bubble location/width from the GOLD FUV images (estimated accuracy: $\sim 1^\circ$ geomagnetic longitude)
 - An intensive manual review of the images & algorithm results is employed to finalize a list of bubbles in which the team has confidence

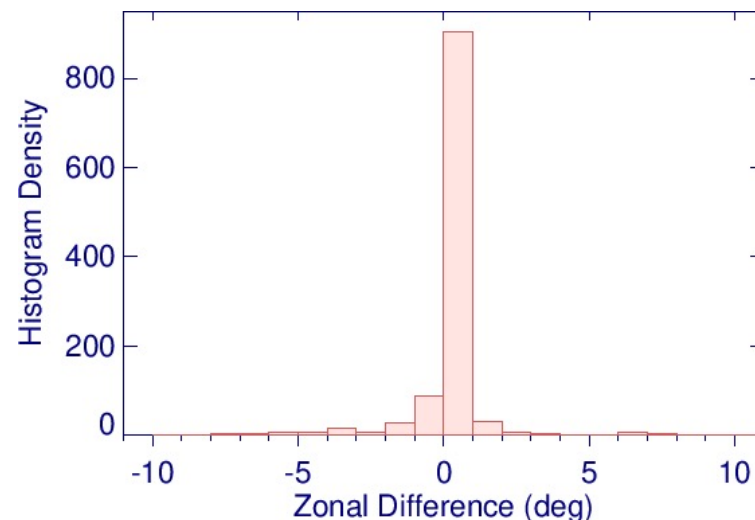
Example: Day 070 of 2020

UCAR colored GOLD image: EPBs identified by automated algorithm shown as white circles



Grayscale versions of the imagery usually provide better contrast for identifying depletions.

1. An automated algorithm from UCAR was used to detect bubbles in GOLD UV images and measure their zonal width.
2. These bubbles were verified via manual inspection. The uncertainties in GOLD bubble location and width were about 0.7° and 1.1° , respectively.
3. TGRS geolocation error was computed as the zonal distance from the GEO to the nearest manually verified GOLD bubble.

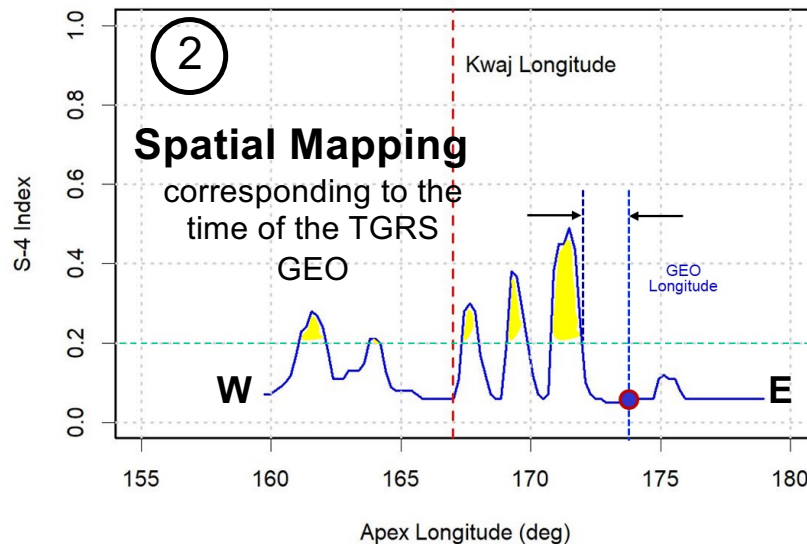
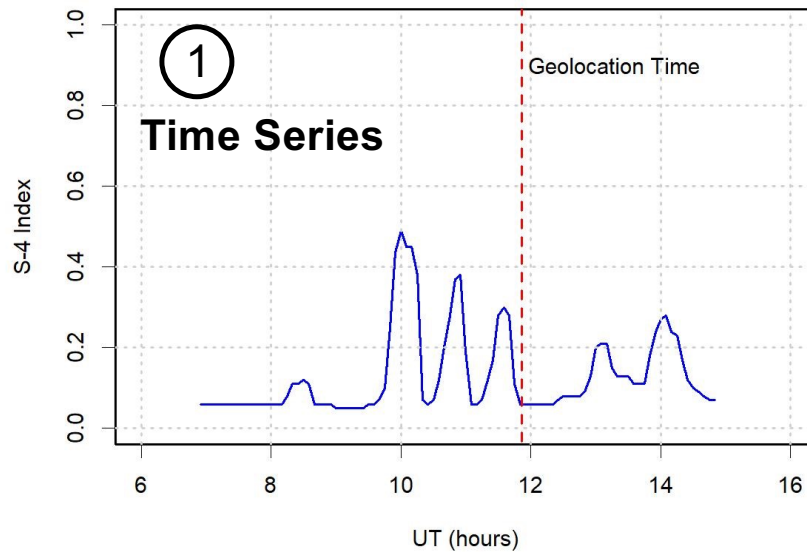


Error Statistics

Error (deg)	Samples	%
All	1107	100.0
< 5	1085	98.0
< 2	1048	94.7
< 1	992	89.6
0	852	77.0

Validation of 1107 TGRS geolocations using GOLD UV images show that 90% are located within 1° longitude from a GOLD bubble.

Kwajalein GEO-Validation for Day 2020/252 Hour 11:52

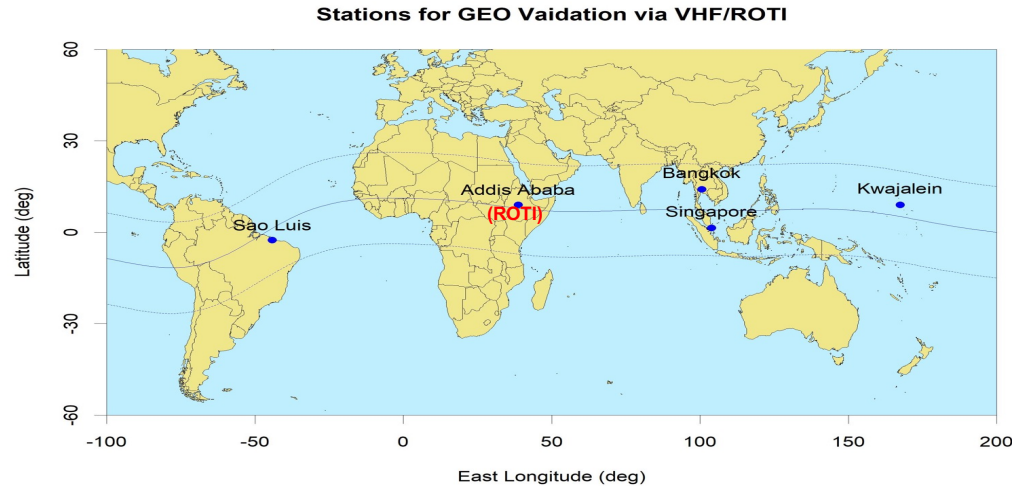


A time-series of S4 from a geostationary satellite link can be used to generate a 1D scintillation structure map in magnetic longitude and subsequently compared with TGRS geolocations:

1. The validation data is a time series of S4 data for one night from a single site location defined by the apex longitude of the ionospheric pierce point of the VHF link.
2. When a geolocation event between 19-24 LT occurs within 5° apex longitude of the site, map the data from time to space by multiplying by average zonal drift & time difference relative to the geolocation time.

$$S4(x_i) = S4(t_i) \times (t_{geo} - t_i) v_d$$

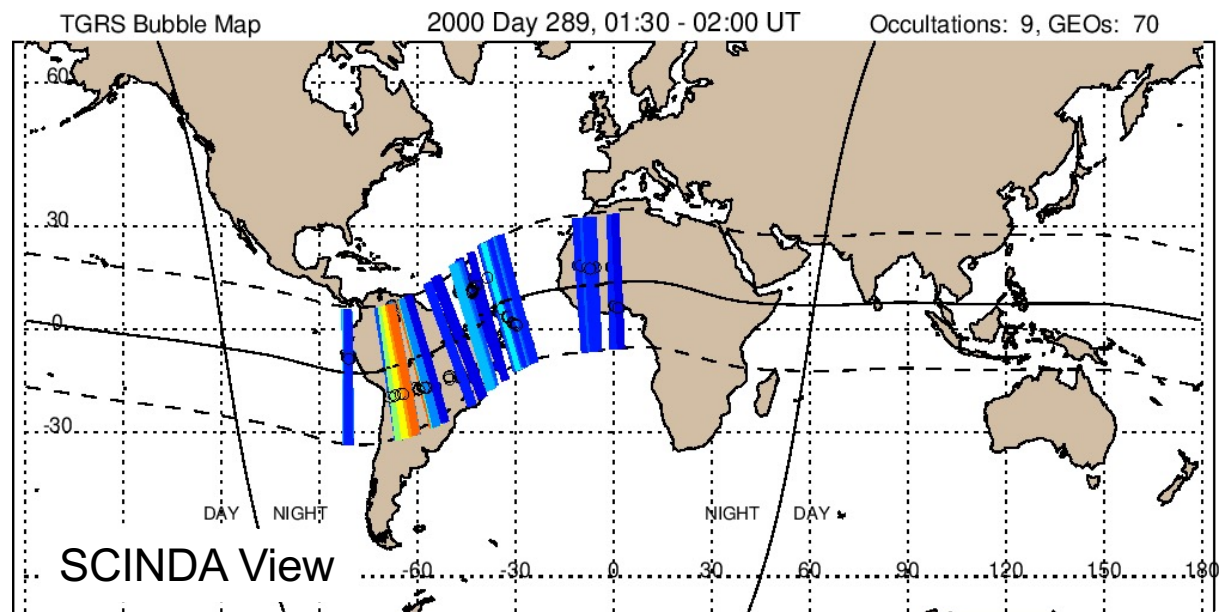
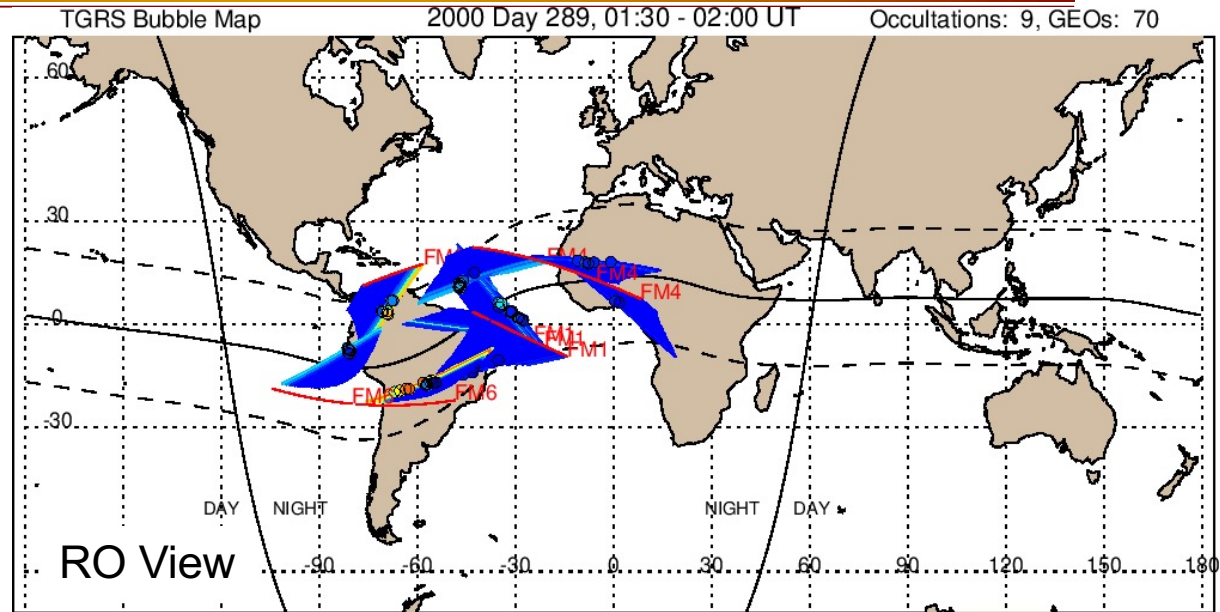
The geolocation error, or miss distance, is defined as the difference between the GEO longitude and the nearest S4 structure above the S4 threshold (0.2)



Errors in Geolocation from VHF/ROTI Validation										
	Sao Luis		Singapore		Bangkok		Kwajalein		Addis Ababa	
Total GEOs	1777	100%	496	100%	387	100%	335	100%	296	100%
Errors < 2-deg	1755	98.8%	484	97.6%	367	94.8%	308	91.9%	290	98.0%
Errors < 1-deg	1714	96.4%	464	93.6%	341	88.1%	282	84.2%	279	94.2%
RMS Error	0.41-deg		0.58-deg		0.81-deg		0.99-deg		0.56-deg	

A validation of more than 3000 TGRS geolocations from five independent measurement sites produced rms errors of less than 1° in longitude (~100 km)₁ at each site.

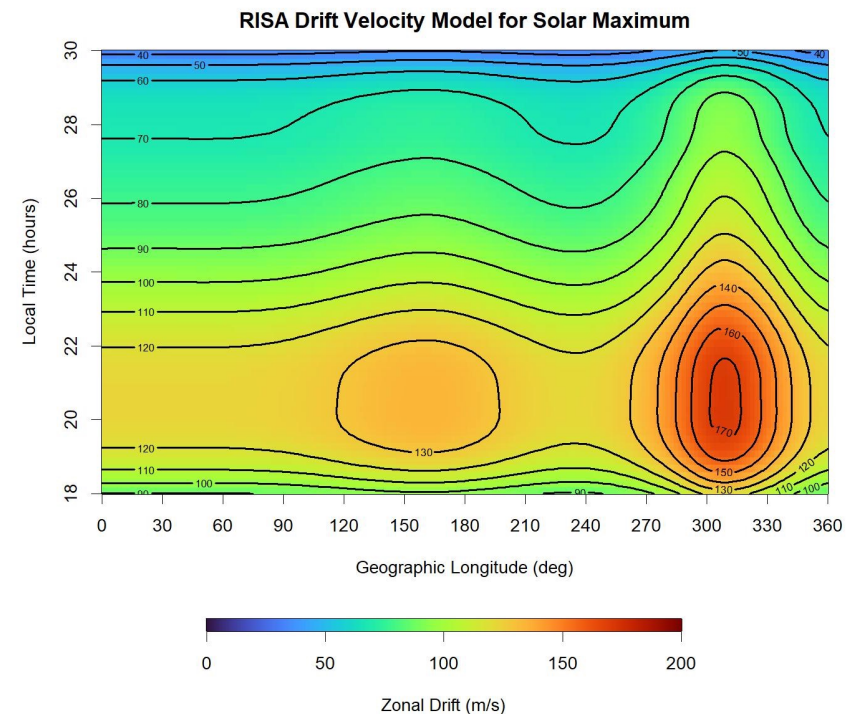
- We have developed a TGRS **Bubble Map Product** to visualize the global distribution of plasma bubbles.
- A separate **Limb-to-Disk Product** extracts quantitative estimates of CkL from the RO S4, and then predicts S4 at other frequencies (UHF).
- This RO data is being merged with ground-based scintillation (SCINDA) to provide next-generation scintillation nowcast/forecast products.



Bubble Persistence and Propagation



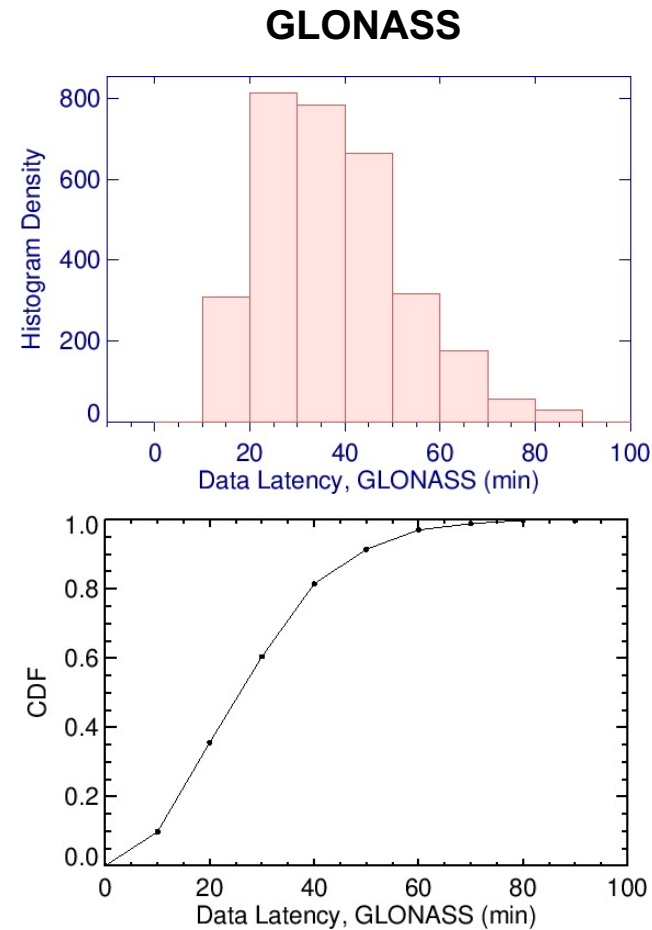
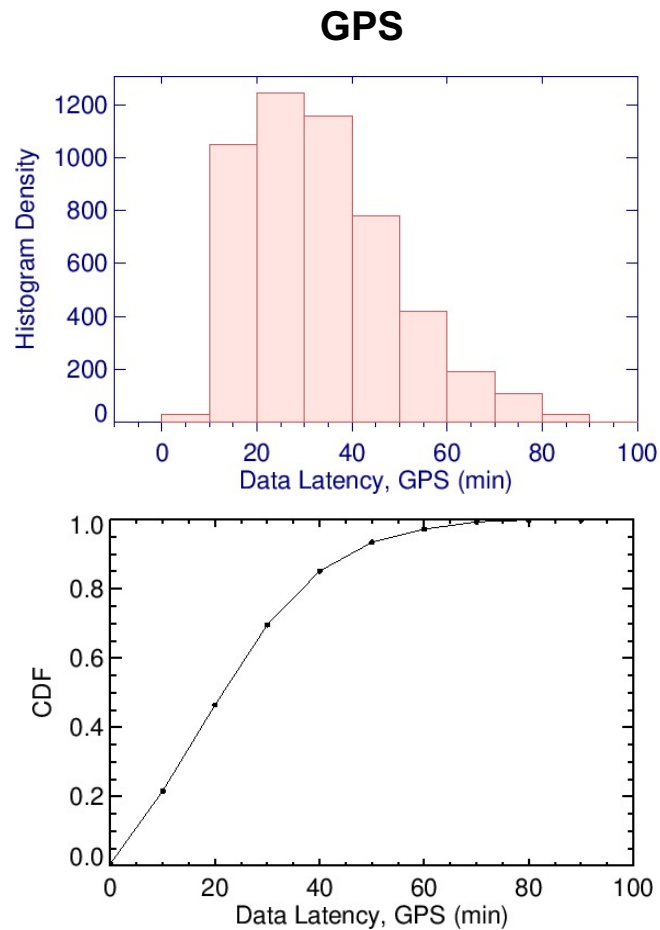
- TGRS detects only bubbles intersected by the RO ray-paths at F-region altitudes, and those for which RO S4 triggers download of high-rate data.
- Once detected, we know that bubbles can still be present (typically for a few hours) even if they are not sampled again by new occultations.
- To improve product “coverage” we allow detected bubbles to persist for a specified time (e.g. 60/90/120 min)
- Old bubbles are propagated to the current time using a climatological model of zonal irregularity drift
- A statistical analysis revealed that persistence is largely unnecessary for prompt data (implying that TGRS detects most bubbles repeatedly), but it’s effective at mitigating coverage loss due to data latency.



TGRS High-Rate Data Latency

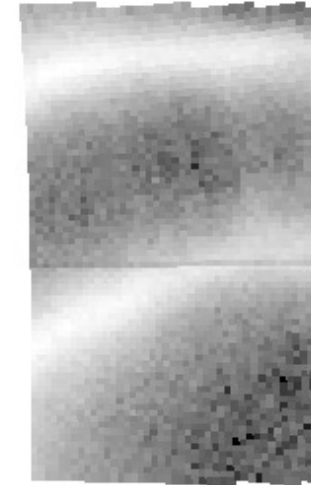
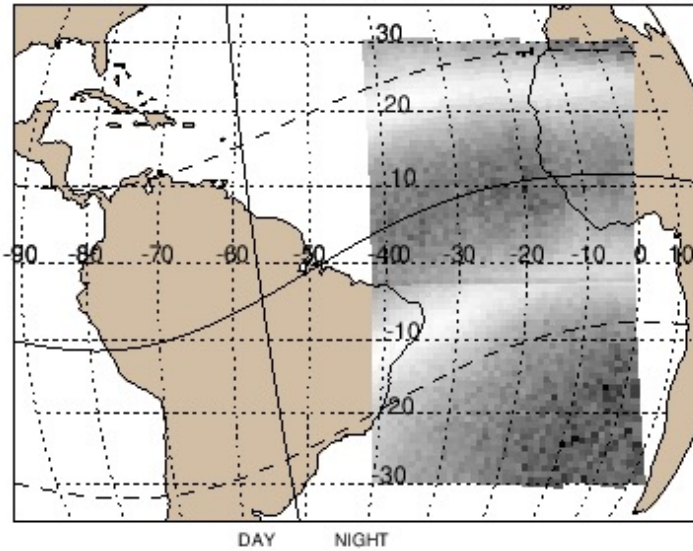


- As expected, data latency has a significant impact on TGRS product coverage
- We *simulated* TGRS data latency as the difference between file completion time provided by UCAR and the central time of the data within each scnPhs file.
- Histograms and cumulative distribution functions for the GPS data (left), and GLONASS data (right) are shown below.



Prompt
Data

TGRS Bubble Map 2022 Day 058, 22:00 UT Occultations: 0, GEOs: 0
 Ingest period: 2022 Day 058, 20:30 - 2022 Day 058, 22:00 UT, Valid time: 2022 Day 058, 22:00 UT

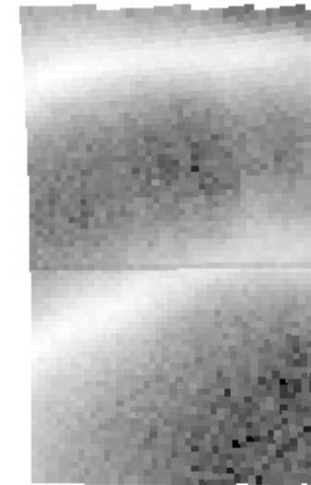
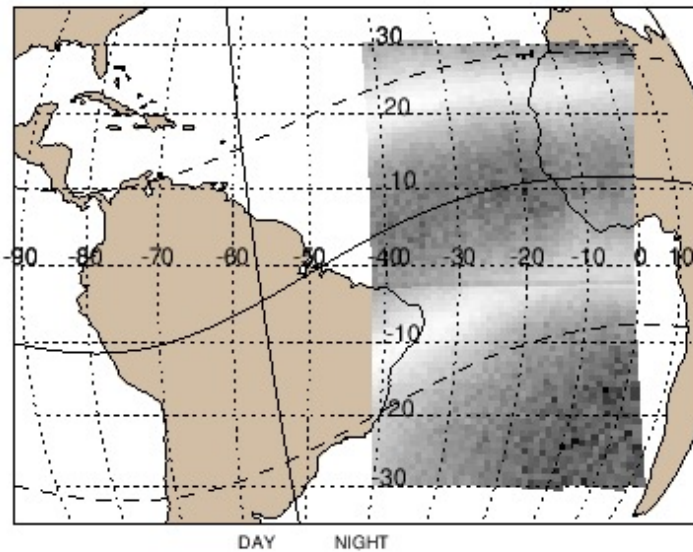


GOLD_L1C_CHA_NI1_2022_058_21_52_v04_r01_c01.nc

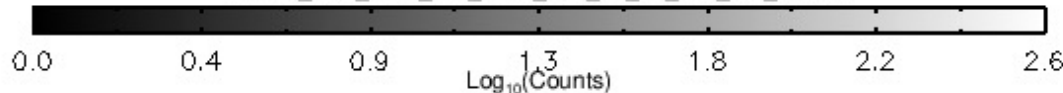
GOLD data is used to determine how much "coverage" the TGRS Bubble Maps provide

With
Simulated
Latency

TGRS Bubble Map 2022 Day 058, 22:00 UT Occultations: 0, GEOs: 0
 Ingest period: 2022 Day 058, 20:30 - 2022 Day 058, 22:00 UT, Valid time: 2022 Day 058, 22:00 UT

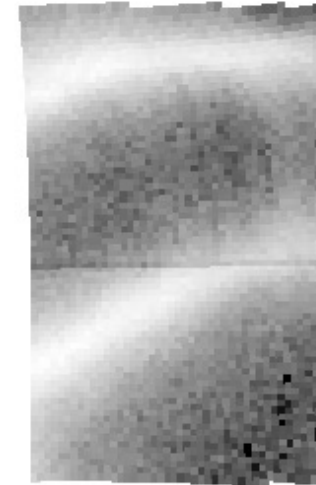
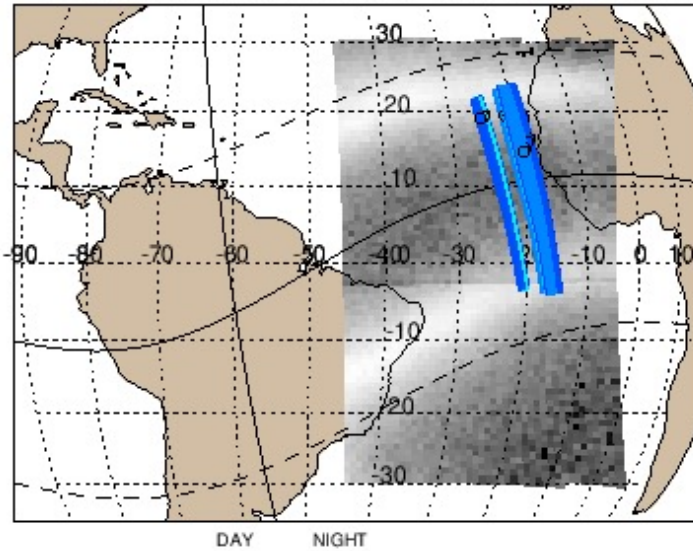


GOLD_L1C_CHA_NI1_2022_058_21_52_v04_r01_c01.nc
 GOLD_L1C_CHB_NI1_2022_058_21_55_v04_r01_c01.nc



Prompt
 Data

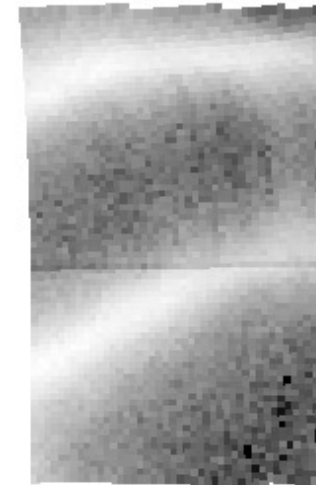
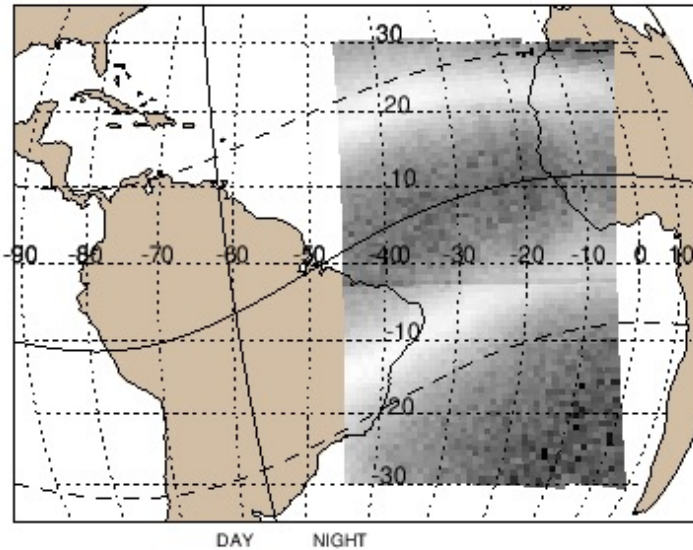
TGRS Bubble Map 2022 Day 058, 22:15 UT Occultations: 2, GEOs: 13
 Ingest period: 2022 Day 058, 20:45 - 2022 Day 058, 22:15 UT, Valid time: 2022 Day 058, 22:15 UT



GOLD_L1C_CHA_NI1_2022_058_22_10_v04_r01_c01.nc

With
 Simulated
 Latency

TGRS Bubble Map 2022 Day 058, 22:15 UT Occultations: 0, GEOs: 0
 Ingest period: 2022 Day 058, 20:45 - 2022 Day 058, 22:15 UT, Valid time: 2022 Day 058, 22:15 UT

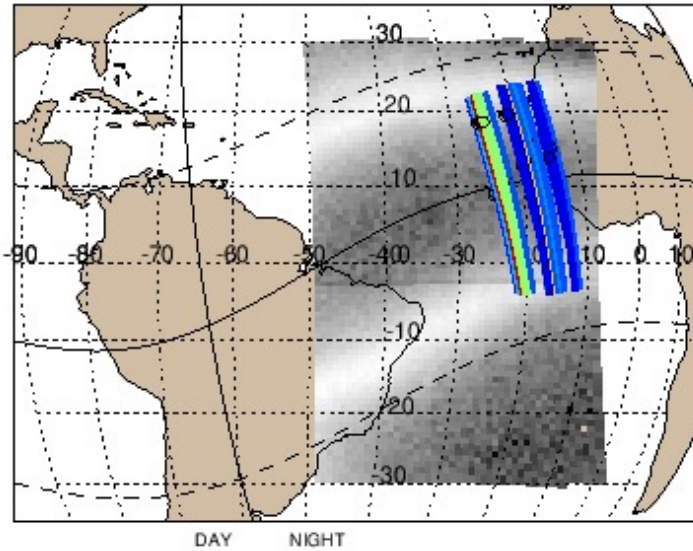


GOLD_L1C_CHA_NI1_2022_058_22_10_v04_r01_c01.nc
 GOLD_L1C_CHB_NI1_2022_058_22_10_v04_r01_c01.nc



Prompt
 Data

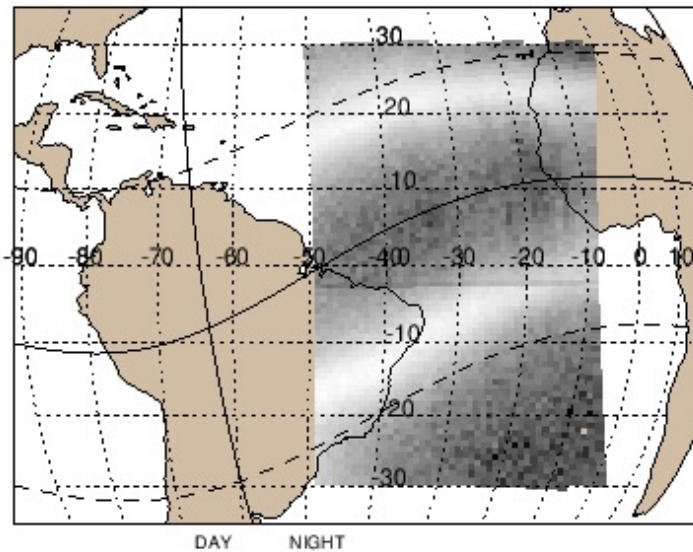
TGRS Bubble Map 2022 Day 058, 22:30 UT Occultations: 3, GEOs: 34
 Ingest period: 2022 Day 058, 21:00 - 2022 Day 058, 22:30 UT, Valid time: 2022 Day 058, 22:30 UT



GOLD_L1C_CHA_NI1_2022_058_22_22_v04_r01_c01.nc

With
 Simulated
 Latency

TGRS Bubble Map 2022 Day 058, 22:30 UT Occultations: 0, GEOs: 0
 Ingest period: 2022 Day 058, 21:00 - 2022 Day 058, 22:30 UT, Valid time: 2022 Day 058, 22:30 UT

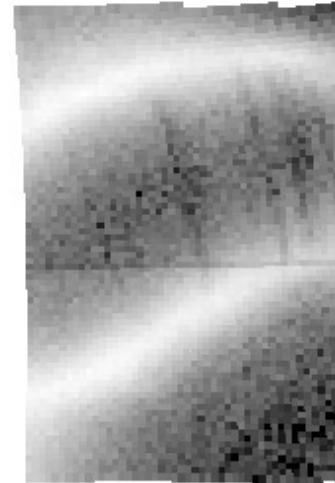
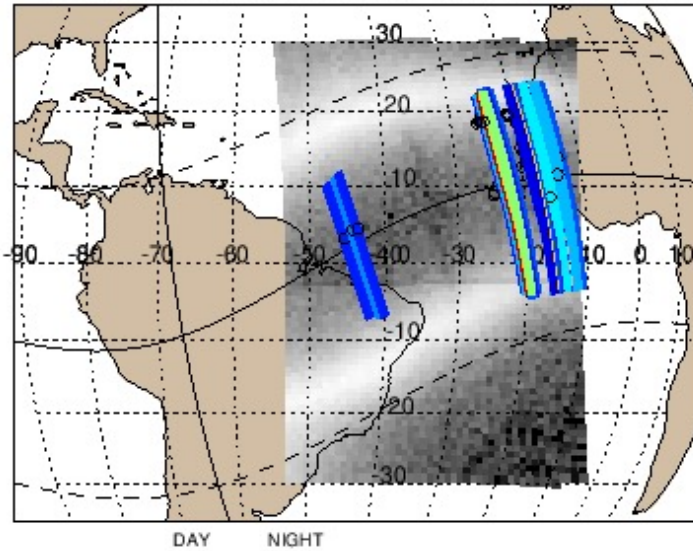


GOLD_L1C_CHA_NI1_2022_058_22_22_v04_r01_c01.nc
 GOLD_L1C_CHB_NI1_2022_058_22_25_v04_r01_c01.nc



Prompt
Data

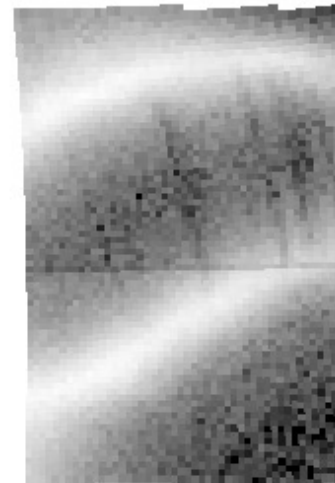
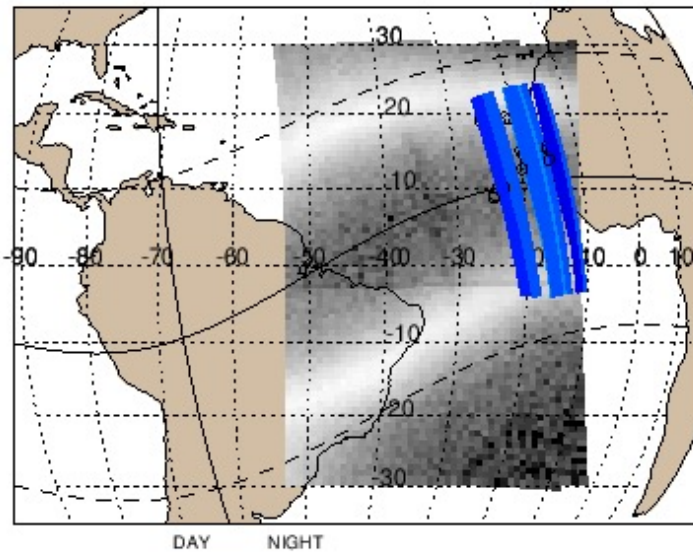
TGRS Bubble Map 2022 Day 058, 22:45 UT Occultations: 6, GEOs: 60
Ingest period: 2022 Day 058, 21:15 - 2022 Day 058, 22:45 UT, Valid time: 2022 Day 058, 22:45 UT



GOLD_L1C_CHA_NI1_2022_058_22_40_v04_r01_c01.nc

With
Simulated
Latency

TGRS Bubble Map 2022 Day 058, 22:45 UT Occultations: 2, GEOs: 24
Ingest period: 2022 Day 058, 21:15 - 2022 Day 058, 22:45 UT, Valid time: 2022 Day 058, 22:45 UT

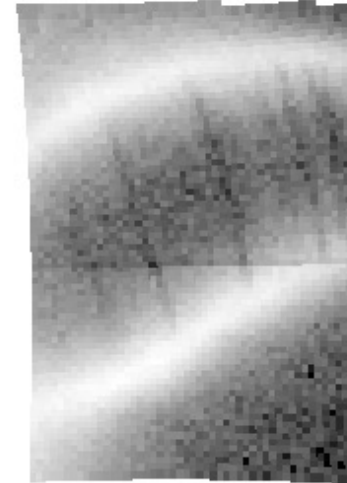
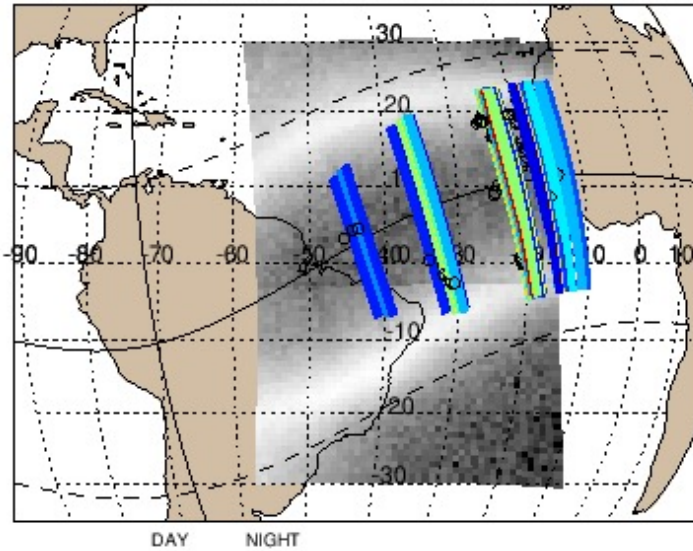


GOLD_L1C_CHA_NI1_2022_058_22_40_v04_r01_c01.nc
GOLD_L1C_CHB_NI1_2022_058_22_40_v04_r01_c01.nc



Prompt
 Data

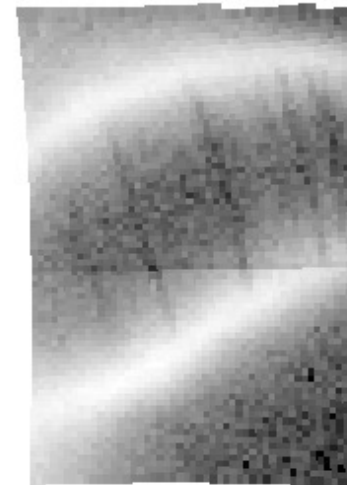
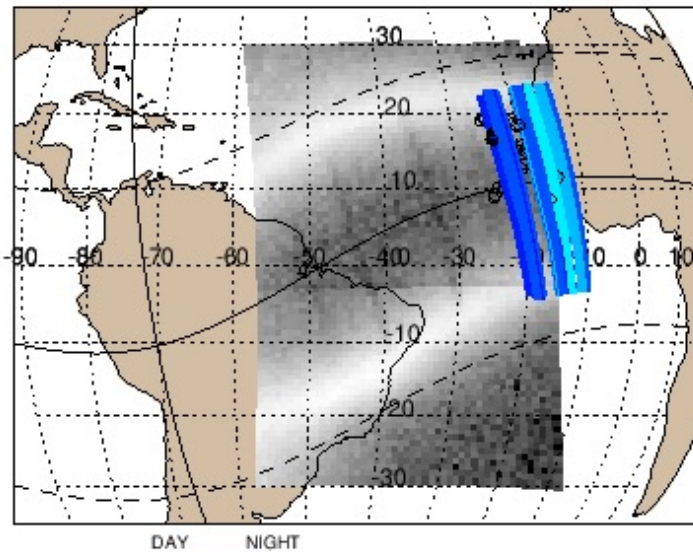
TGRS Bubble Map 2022 Day 058, 23:00 UT Occultations: 10, GEOs: 94
 Ingest period: 2022 Day 058, 21:30 - 2022 Day 058, 23:00 UT, Valid time: 2022 Day 058, 23:00 UT



GOLD_L1C_CHA_NI1_2022_058_22_52_v04_r01_c01.nc

With
 Simulated
 Latency

TGRS Bubble Map 2022 Day 058, 23:00 UT Occultations: 4, GEOs: 47
 Ingest period: 2022 Day 058, 21:30 - 2022 Day 058, 23:00 UT, Valid time: 2022 Day 058, 23:00 UT

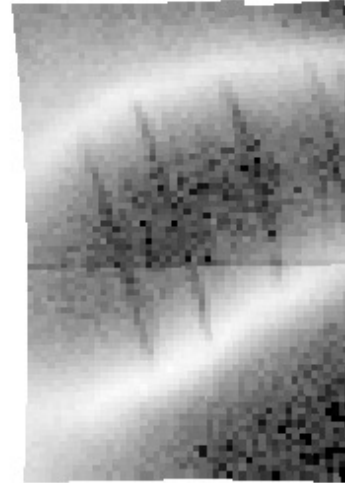
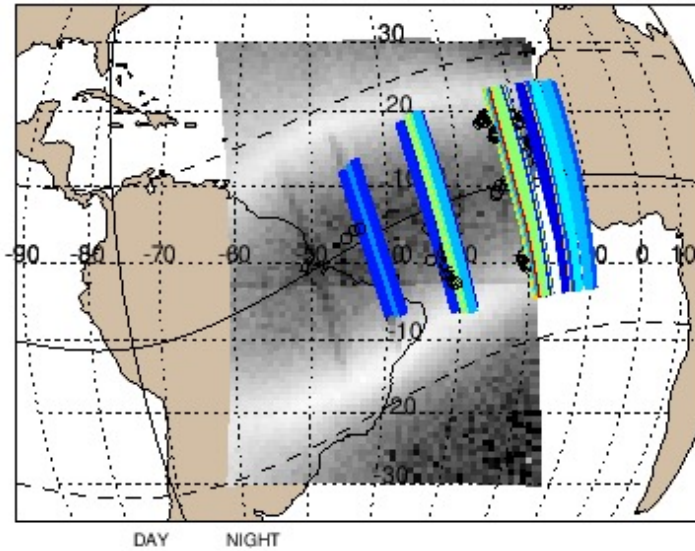


GOLD_L1C_CHA_NI1_2022_058_22_52_v04_r01_c01.nc
 GOLD_L1C_CHB_NI1_2022_058_22_55_v04_r01_c01.nc



Prompt
Data

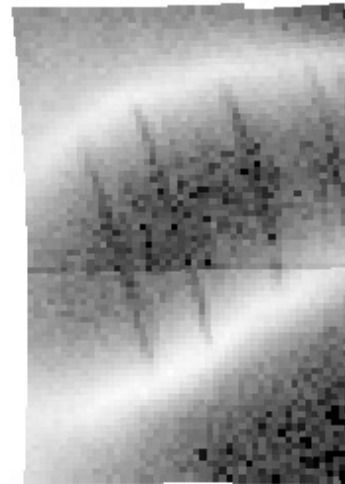
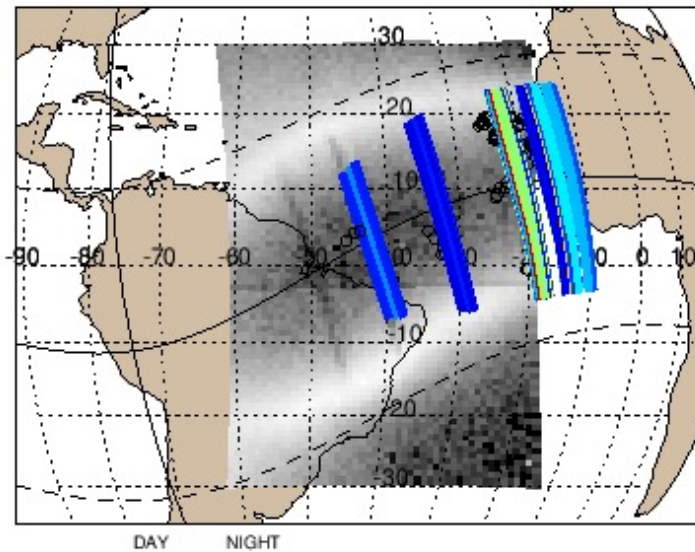
TGRS Bubble Map 2022 Day 058, 23:15 UT Occultations: 10, GEOs: 94
 Ingest period: 2022 Day 058, 21:45 - 2022 Day 058, 23:15 UT, Valid time: 2022 Day 058, 23:15 UT



GOLD_L1C_CHA_NI1_2022_058_23_10_v04_r01_c01.nc

With
Simulated
Latency

TGRS Bubble Map 2022 Day 058, 23:15 UT Occultations: 8, GEOs: 71
 Ingest period: 2022 Day 058, 21:45 - 2022 Day 058, 23:15 UT, Valid time: 2022 Day 058, 23:15 UT

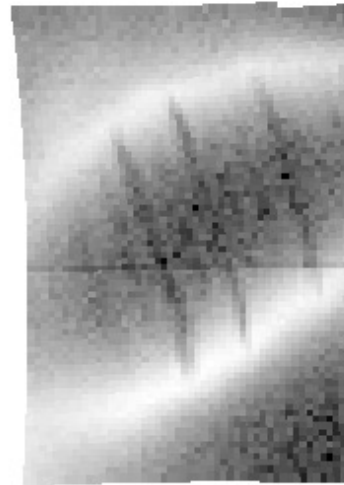
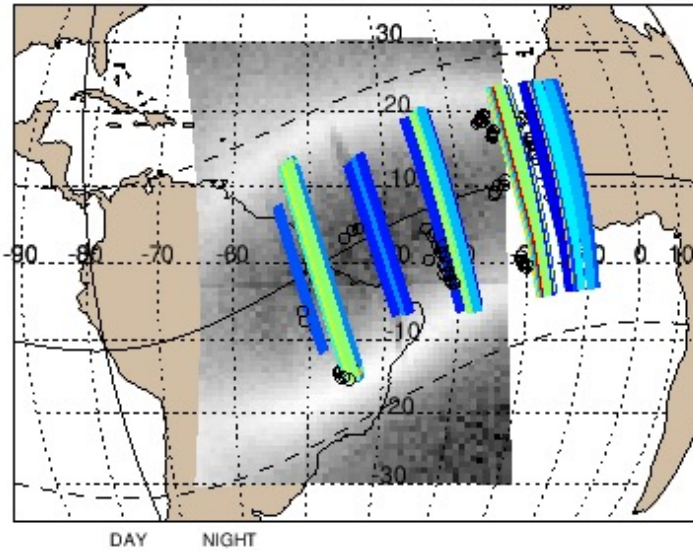


GOLD_L1C_CHA_NI1_2022_058_23_10_v04_r01_c01.nc
 GOLD_L1C_CHB_NI1_2022_058_23_10_v04_r01_c01.nc



Prompt
 Data

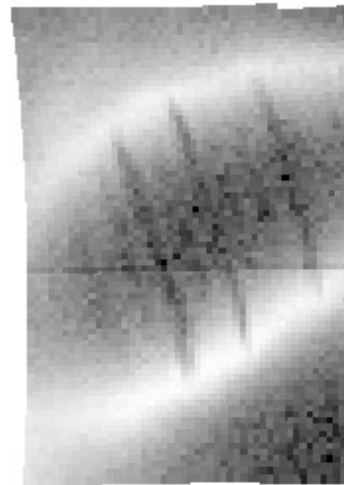
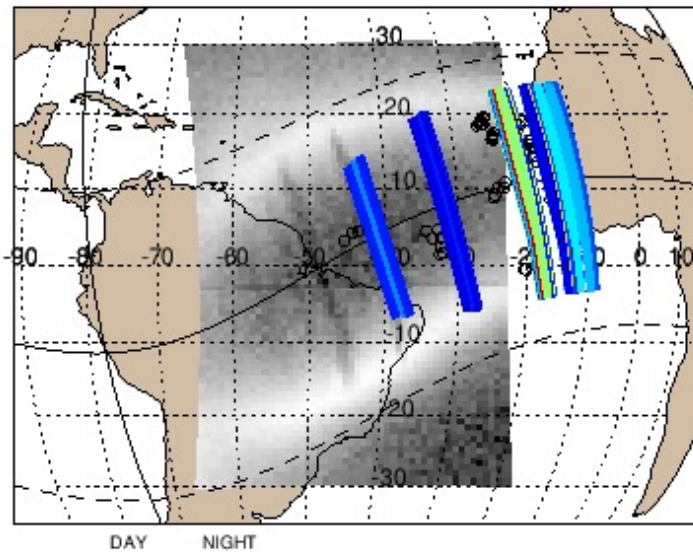
TGRS Bubble Map 2022 Day 058, 23:30 UT Occultations: 14, GEOs: 109
 Ingest period: 2022 Day 058, 22:00 - 2022 Day 058, 23:30 UT, Valid time: 2022 Day 058, 23:30 UT



GOLD_L1C_CHA_NI1_2022_058_23_22_v04_r01_c01.nc

With
 Simulated
 Latency

TGRS Bubble Map 2022 Day 058, 23:30 UT Occultations: 8, GEOs: 71
 Ingest period: 2022 Day 058, 22:00 - 2022 Day 058, 23:30 UT, Valid time: 2022 Day 058, 23:30 UT

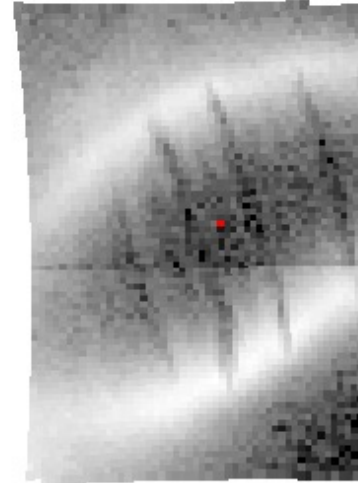
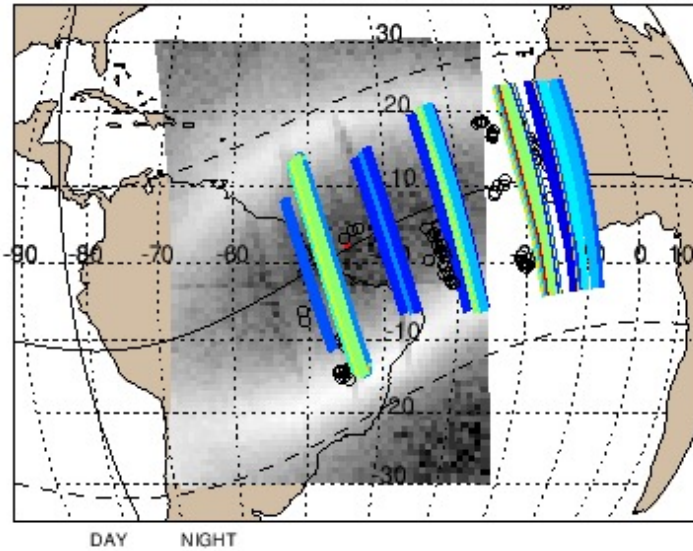


GOLD_L1C_CHA_NI1_2022_058_23_22_v04_r01_c01.nc
 GOLD_L1C_CHB_NI1_2022_058_23_25_v04_r01_c01.nc



Prompt
Data

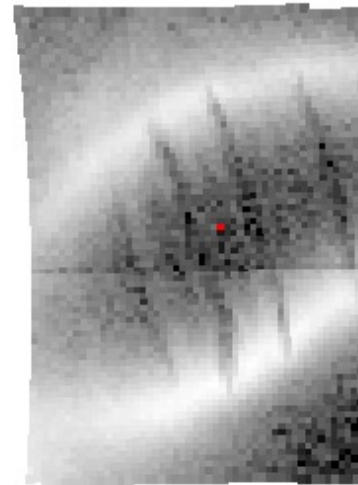
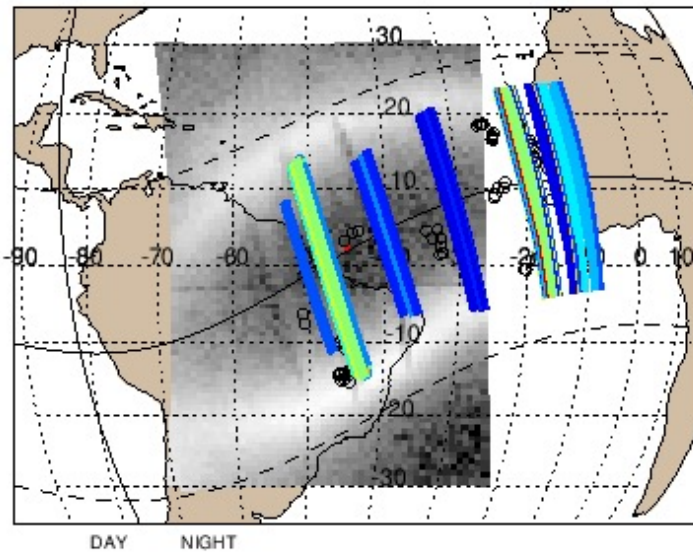
TGRS Bubble Map 2022 Day 058, 23:45 UT Occultations: 13, GEOs: 96
 Ingest period: 2022 Day 058, 22:15 - 2022 Day 058, 23:45 UT, Valid time: 2022 Day 058, 23:45 UT



GOLD_L1C_CHA_NI1_2022_058_23_40_v04_r01_c01.nc

With
Simulated
Latency

TGRS Bubble Map 2022 Day 058, 23:45 UT Occultations: 11, GEOs: 73
 Ingest period: 2022 Day 058, 22:15 - 2022 Day 058, 23:45 UT, Valid time: 2022 Day 058, 23:45 UT

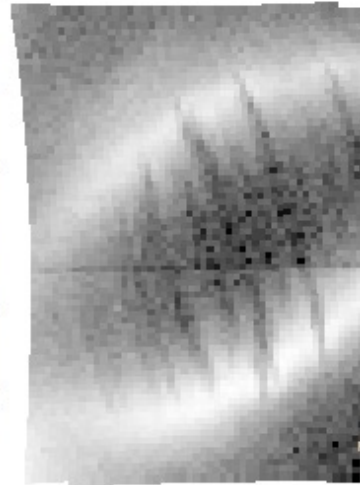
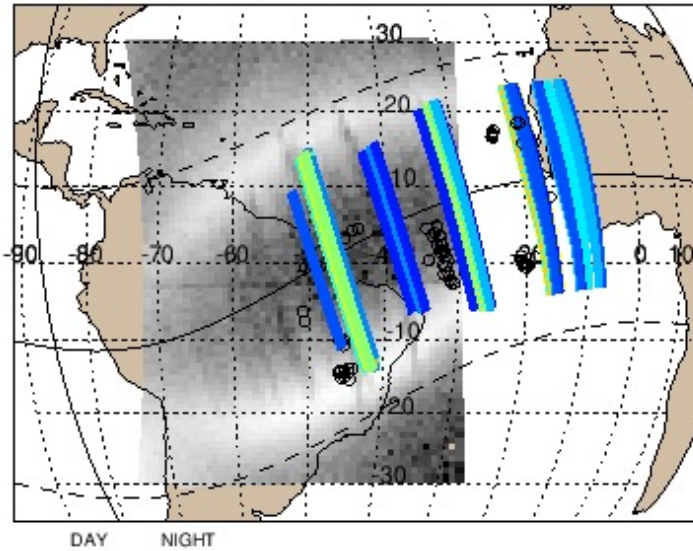


GOLD_L1C_CHA_NI1_2022_058_23_40_v04_r01_c01.nc
 GOLD_L1C_CHB_NI1_2022_058_23_40_v04_r01_c01.nc



Prompt
Data

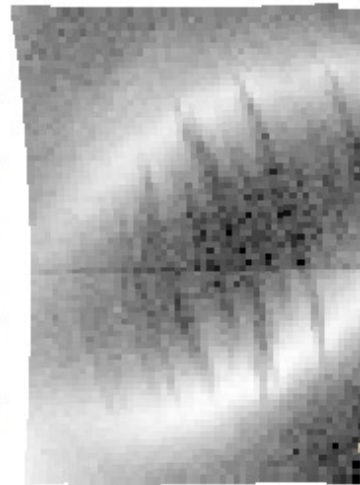
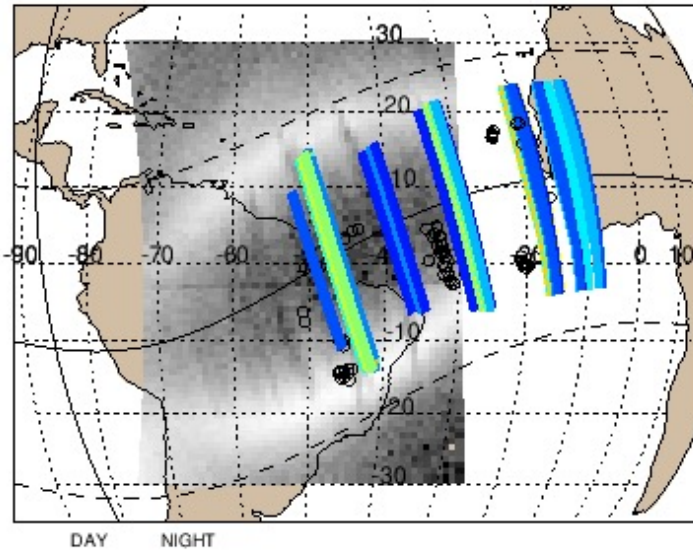
TGRS Bubble Map 2022 Day 058, 24:00 UT Occultations: 11, GEOs: 75
 Ingest period: 2022 Day 058, 22:30 - 2022 Day 058, 24:00 UT, Valid time: 2022 Day 058, 24:00 UT



GOLD_L1C_CHA_NI1_2022_058_23_52_v04_r01_c01.nc

With
Simulated
Latency

TGRS Bubble Map 2022 Day 058, 24:00 UT Occultations: 11, GEOs: 75
 Ingest period: 2022 Day 058, 22:30 - 2022 Day 058, 24:00 UT, Valid time: 2022 Day 058, 24:00 UT

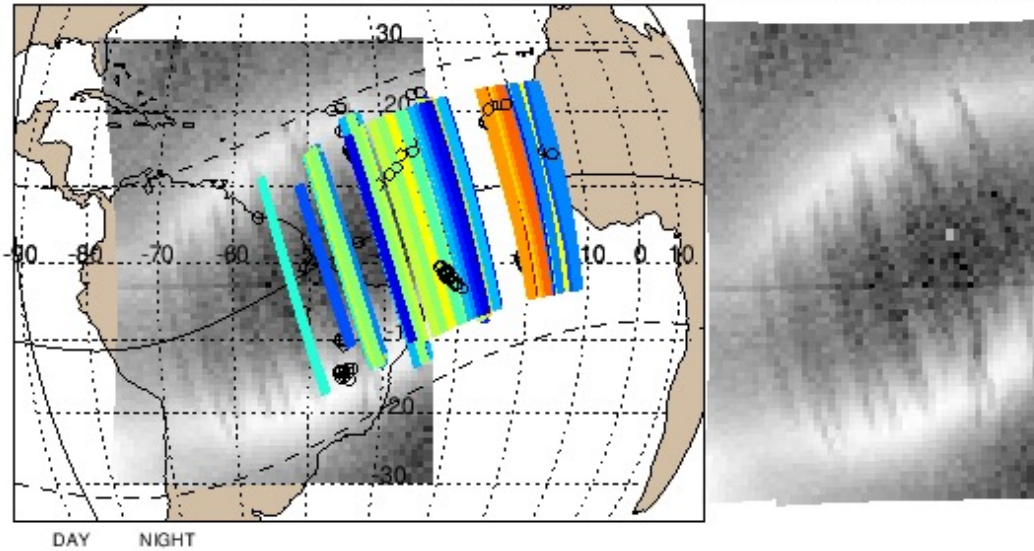


GOLD_L1C_CHA_NI1_2022_058_23_52_v04_r01_c01.nc
 GOLD_L1C_CHB_NI1_2022_058_23_55_v04_r01_c01.nc



Prompt
Data

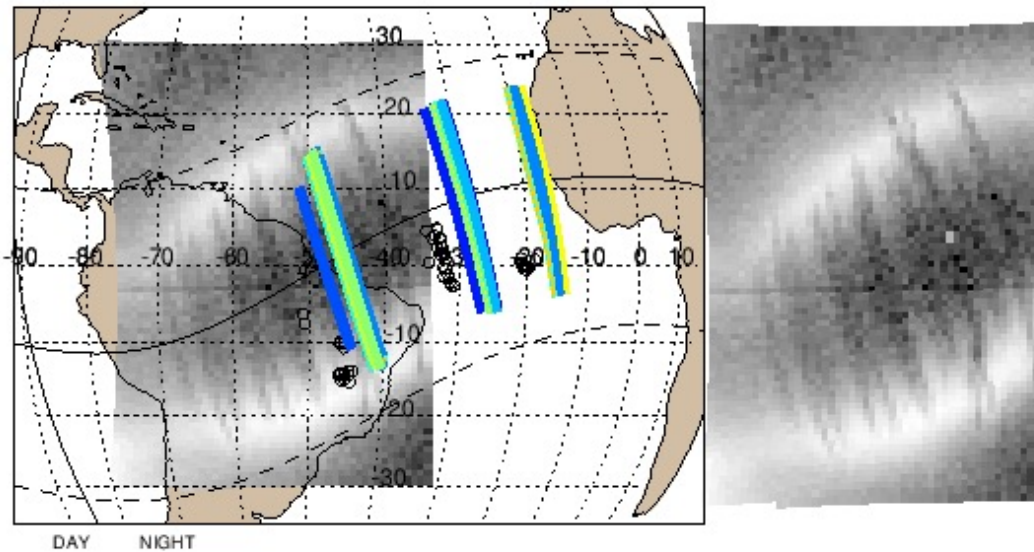
TGRS Bubble Map 2022 Day 059, 00:15 UT Occultations: 15, GEOs: 121
 Ingest period: 2022 Day 058, 22:45 - 2022 Day 059, 00:15 UT, Valid time: 2022 Day 059, 00:15 UT



GOLD_L1C_CHA_NI1_2022_059_00_10_v04_r01_c01.nc

With
Simulated
Latency

TGRS Bubble Map 2022 Day 059, 00:15 UT Occultations: 9, GEOs: 49
 Ingest period: 2022 Day 058, 22:45 - 2022 Day 059, 00:15 UT, Valid time: 2022 Day 059, 00:15 UT

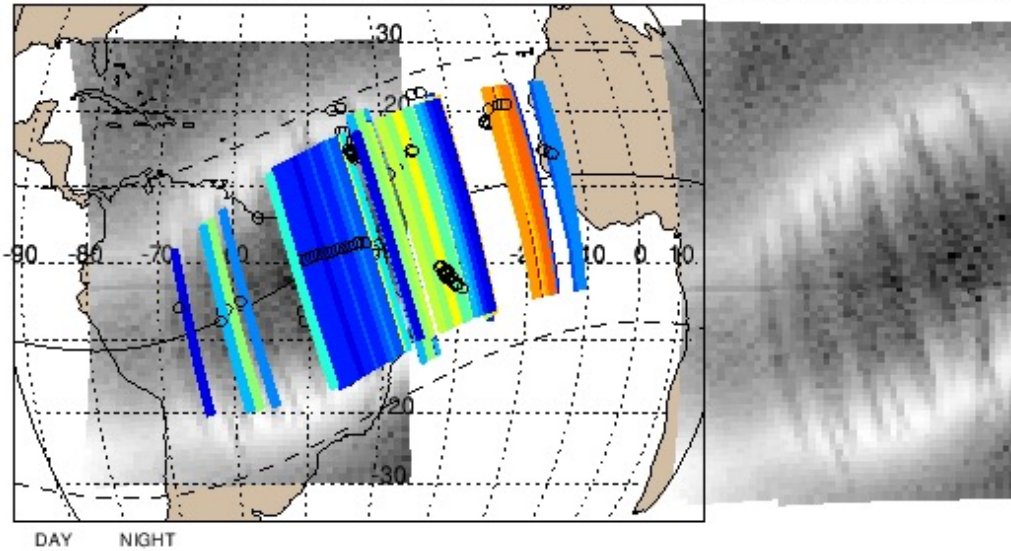


GOLD_L1C_CHA_NI1_2022_059_00_10_v04_r01_c01.nc
 GOLD_L1C_CHB_NI1_2022_059_00_10_v04_r01_c01.nc



Prompt
Data

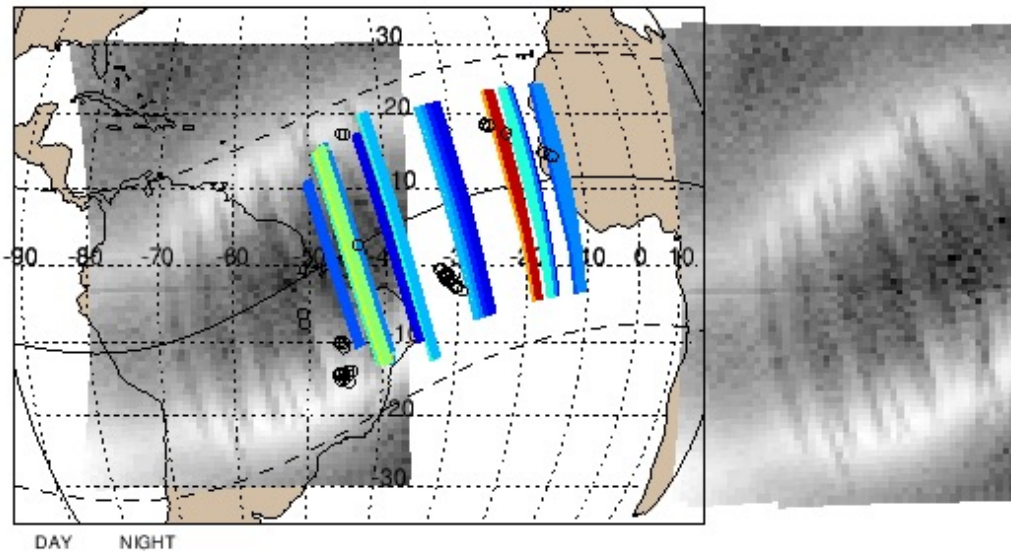
TGRS Bubble Map 2022 Day 059, 00:30 UT Occultations: 15, GEOs: 128
 Ingest period: 2022 Day 058, 23:00 - 2022 Day 059, 00:30 UT, Valid time: 2022 Day 059, 00:30 UT



GOLD_L1C_CHA_NI1_2022_059_00_28_v04_r01_c01.nc

With
Simulated
Latency

TGRS Bubble Map 2022 Day 059, 00:30 UT Occultations: 7, GEOs: 49
 Ingest period: 2022 Day 058, 23:00 - 2022 Day 059, 00:30 UT, Valid time: 2022 Day 059, 00:30 UT

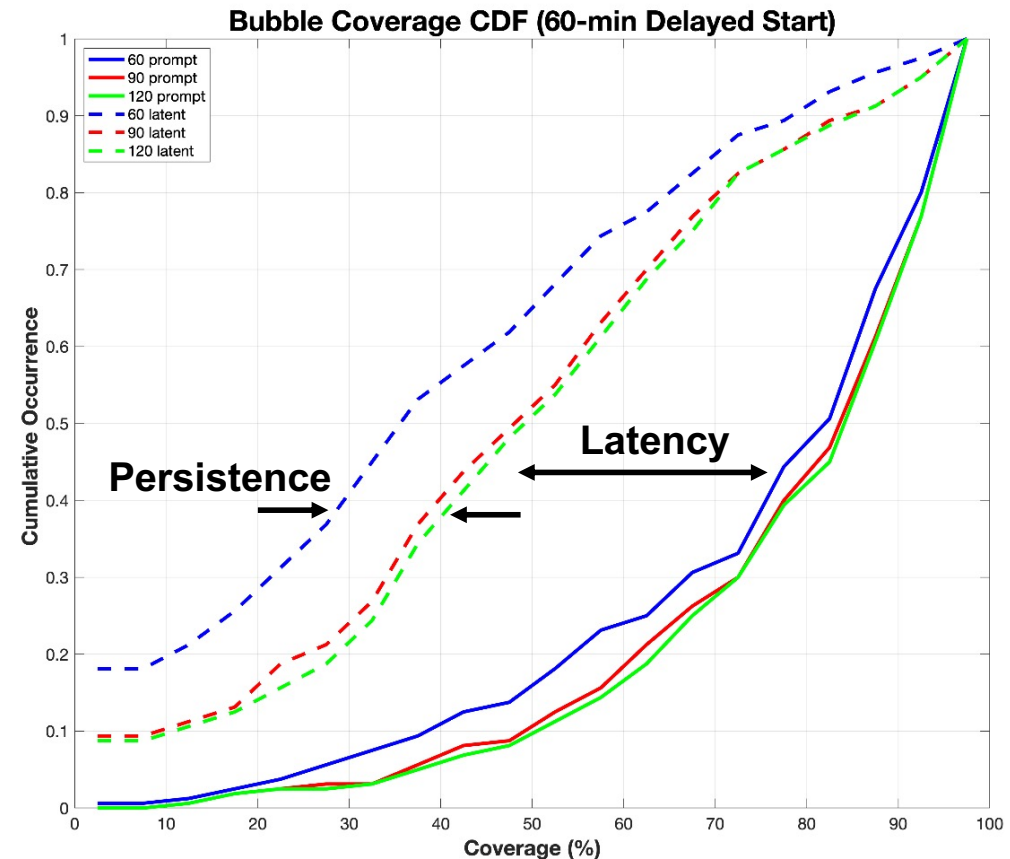


GOLD_L1C_CHA_NI1_2022_059_00_28_v04_r01_c01.nc
 GOLD_L1C_CHB_NI1_2022_059_00_25_v04_r01_c01.nc



- The cumulative distribution function below provides a summary of the coverage performance for different values of latency and persistence
- On average, **80% bubble coverage** (relative to GOLD) is obtained 90% of the time with prompt data, but only 50% of the time with latent data.

- The large separation between the prompt (solid) and latent (dashed) curves demonstrates the performance gap caused by data latency
- The lesser separation within each group of curves depicts differences due to persistence; for latent data the advantage of using at least 90 min persistence is clear



Real-Time Processing Schedule

Cron (minutes past the hour): 10, 25, 40, 55

Fetch from UCAR

Fetch scnPhs files that have changed since previous fetch, purge files older than 3 hours

Cron (minutes past the hour): 0, 15, 30, 45

TGRS Geolocation

Process GEOs for all occultations with data less than 3 hours old

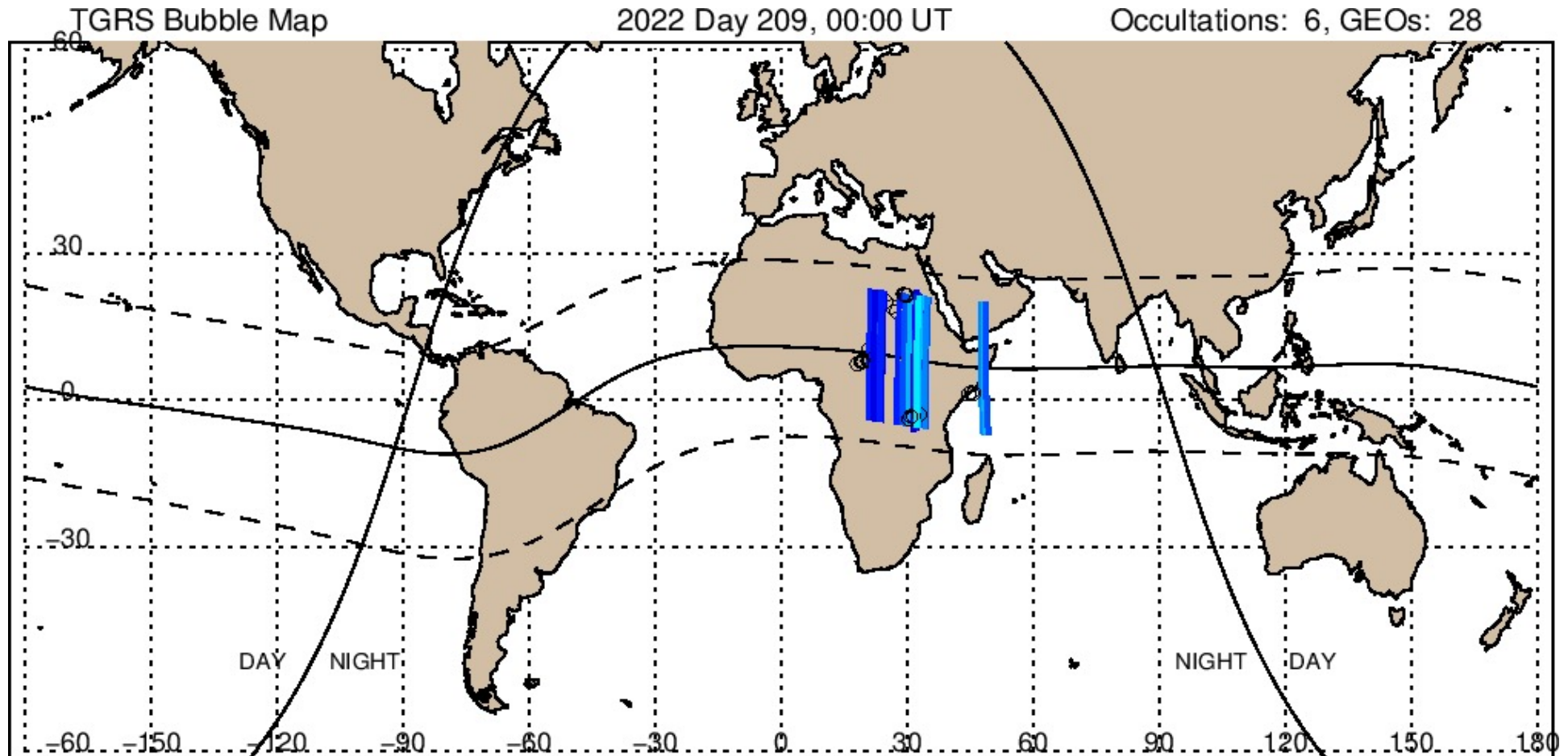


Valid Time

Bubble Map

Ingest all GEOs within **90 min** of the Valid Time

Real-Time Output – 28 July, 2022



90 Minute Persistence

Bubbles colored by RO S4

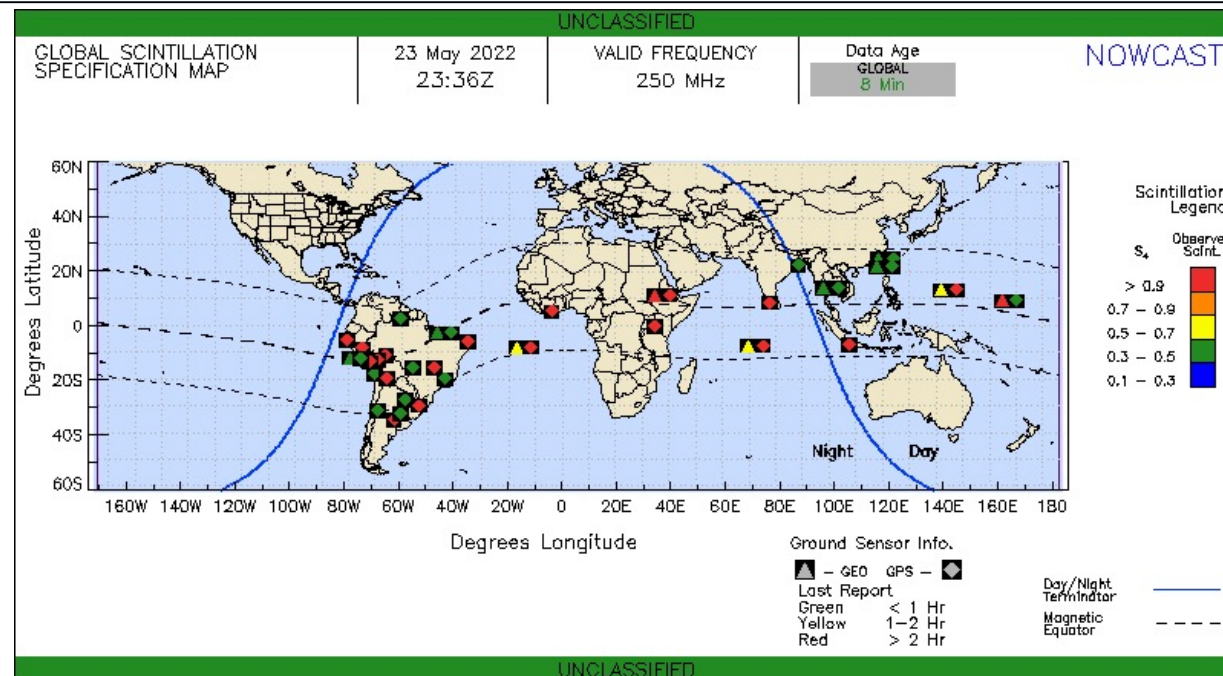
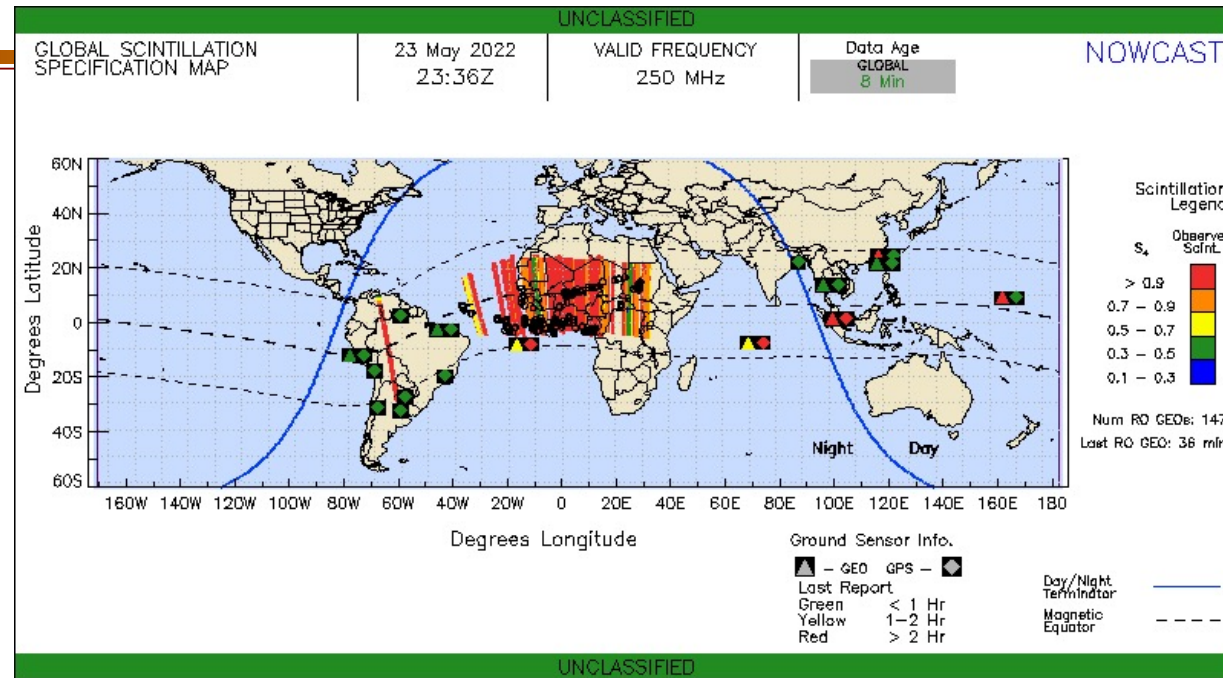
Real-Time SCINDA Product



RO +
 Ground-based
 UHF/GPS

Significant
 improvement
 in coverage

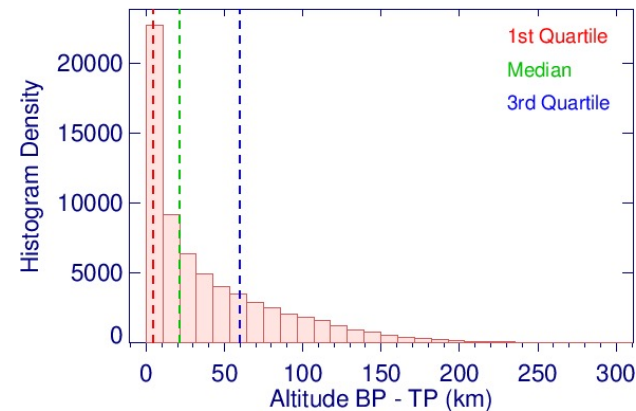
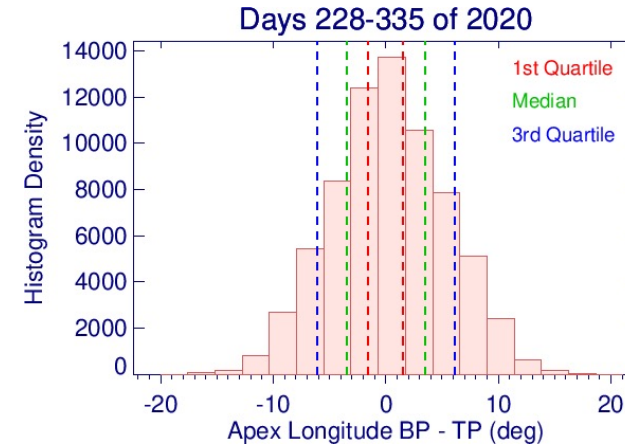
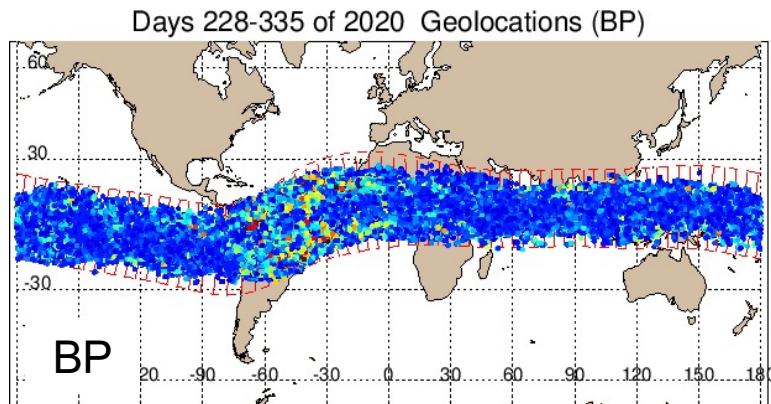
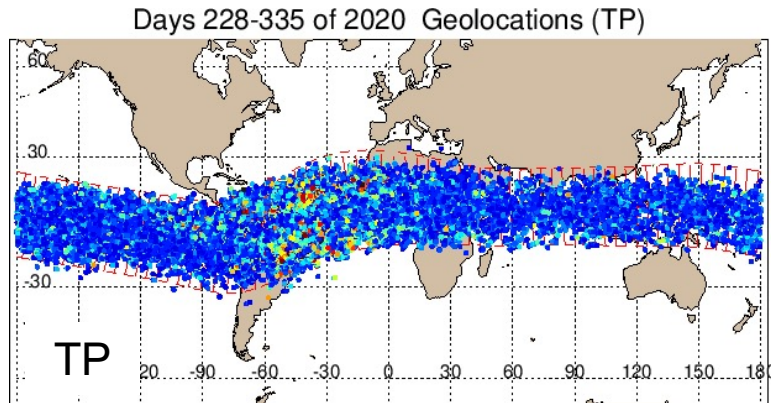
Bubbles colored
 by L2D S4



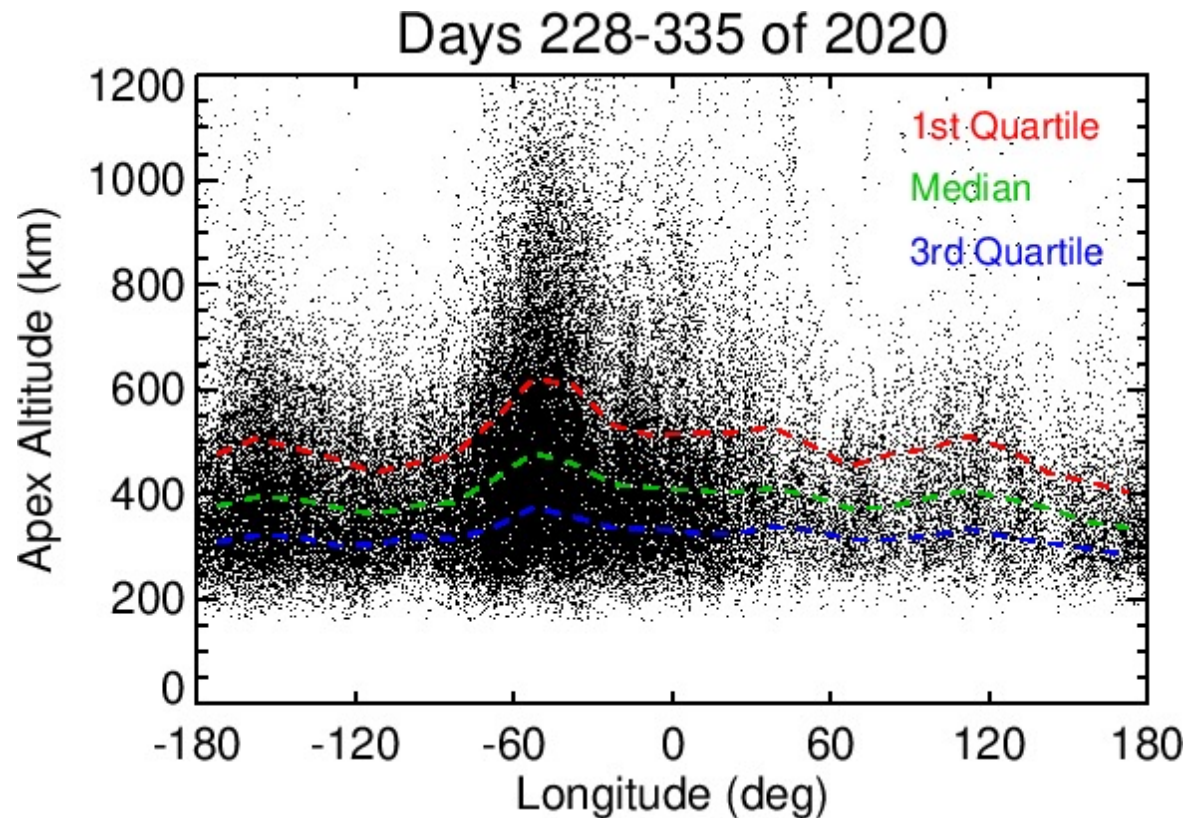
Only Ground-based
 UHF/GPS

Many sensors
 out of service,
 ocean regions
 poorly sampled

On the Tangent Point Assumption



- Studies in the literature often assume irregularities are located near the tangent point. While this is generally not true, for climatological studies the errors may average out.
- On average, RO scintillation *is* most often due to bubbles near the tangent point, but the spread of the distribution is significant. A bubble causing RO scintillation for COSMIC-2 can reside up to **15° distant** from (and up to **200 km above**) the tangent point.



Geolocation apex altitudes show **4-cycle pattern of irregularity occurrence**. Bubbles rise highest over the South Atlantic magnetic anomaly, least high over the Asia sector.

A similar study that assumed irregularities were located at the tangent point (TP) would be biased low, because the actual penetration altitude is always higher than TP altitude.

Conclusions



- Under the COSMIC-2 Calibration/Validation program, we developed a TGRS Geolocation Product to identify the location of irregularities that produce scintillation along COSMIC-2 ray paths to GPS and GLONASS satellites.
- Not all bubbles are detected by TGRS: only those intersected by the RO ray-paths at F-region altitudes, and those for which RO S4 triggers download of high-rate data.
- Validation of > 1100 TGRS geolocations using GOLD UV images show that **90% are located within 1° longitude of a GOLD bubble**. The uncertainties in GOLD bubble location and width are 0.7° and 1.1°, respectively.
- The wide context from GOLD sees more bubbles within the instrument's footprint (South America/Atlantic sector only), but TGRS is able to detect some bubbles that GOLD cannot see. TGRS provides the locations of bubbles globally.
- The **Bubble Map Product** demarcates bubble boundaries, while a separate **Limb-to-Disk algorithm** provides quantitative scintillation strength along typical ground user geometry (vertical propagation).
- We simulated latency to establish coverage/refresh of the Bubble Map Product when operating in real-time conditions. On average, **80% bubble coverage** (relative to GOLD) **is obtained 90% of the time with prompt data, but only 50% of the time with latent data.**